

DOKUZ EYLÜL UNIVERSITY
GRADUATE SCHOOL OF NATURAL AND APPLIED SCIENCES

**DESIGN AND IMPLEMENTATION OF A
WIRELESS TELEMETRY SYSTEM FOR A
SOLAR RACE CAR**

by
Eren GÜL

September, 2015
İZMİR

**DESIGN AND IMPLEMENTATION OF A
WIRELESS TELEMETRY SYSTEM FOR A
SOLAR RACE CAR**

**A Thesis Submitted to the
Graduate School of Natural and Applied Sciences of Dokuz Eylül University
In Partial Fulfillment of the Requirements for the Degree of Master of
Science in Mechatronics Engineering**

**by
Eren GÜL**

**September, 2015
İZMİR**

M.Sc THESIS EXAMINATION RESULT FORM

We have read the thesis entitled **“DESIGN AND IMPLEMENTATION OF A WIRELESS TELEMETRY SYSTEM FOR A SOLAR RACE CAR”** completed by **EREN GÜL** under supervision of **ASSIST. PROF. DR. AYTAÇ GÖREN** and we certify that in our opinion it is fully adequate, in scope and in quality, as a thesis for the degree of Master of Science.



Assist. Prof. Dr. Aytaç GÖREN

Supervisor



Prof. Dr. Zeki KIRAL

(Jury Member)



Assoc. Prof. Dr. Bülent Mustafa İSTEN

(Jury Member)



Prof. Dr. Ayşe OKUR

Director

Graduate School of Natural and Applied Sciences

ACKNOWLEDGEMENTS

I would like to thank to my advisor Assist. Prof. Dr. Aytaç GÖREN for his guidance and supports throughout the project.

I thank to Ministry of Science, Industry and Technology of Republic of Turkey for their support for the thesis with the project number 0065.STZ.2013-1. I thank to CMS Jant ve Makina Sanayi A.Ş. and Özgür Yavuz TOPÇUOĞLU and Ömer Burak ÇE for their support and guidance for this project.

I thank to Destek Automation and Osman KORKUT for their technical support and understanding throughout the project.

I thank to Erdem YALKIN and Volkan ARIKAN for their technical support during the static experiments in the mechanical laboratory.

I thank to my parents for their support and understanding.

I would like to thank to my dear wife Merve UÇAR GÜL for her understanding and support during the project and during extra work hours at home.

Eren GÜL

DESIGN AND IMPLEMENTATION OF A WIRELESS TELEMETRY SYSTEM FOR A SOLAR RACE CAR

ABSTRACT

In this research a telemetry system was designed, produced and tested. This system measures the strain and acceleration then transmits this data to a logger computer with wireless communication. Mainly, this research is based on measuring the dynamic local loads on a car rim.

The local measurements that are taken with this telemetry system can help the mechanical designer to make their designs more strong, more economic and lighter.

This telemetry system includes two parts. One of them is the measuring and transmitting circuit and the other is receiving circuit. On the measurement circuit there are four half-bridge strain gauge inputs, an accelerometer that is located in the middle of the circuit and a transceiver for data transmission. Measurement circuit includes an instrumentation amplifier for strain measurements. In this circuit, digital potentiometers are used for automatic calibration, offset settings and gain selections. Digital switches are used for strain gage selection.

The circuits are designed in Proteus. Software of the PIC microcontroller is written in HITECH C. And the user interface is created in Microsoft Visual Studio.

System was tested and calibrated on a universal testing machine. Then, the telemetry system was tested on the solar race car -SOLARIS of Dokuz Eylül University- on the real road conditions.

Keywords: Telemetry, strain measurement, data logger

GÜNEŞ ENERJİLİ YARIŞ ARABASI İÇİN UZAKTAN KABLOSUZ ÖLÇÜM SİSTEMİ TASARIMI VE UYGULAMASI

ÖZ

Bu araştırmada bir telemetri sistemi tasarlanmış, üretilmiş ve test edilmiştir. Bu sistem uzama ve ivme verilerini ölçer ve bu verileri kablosuz haberleşme ile bir veri depolama bilgisayarına iletir. Esas olarak, bu çalışma araç jantları üzerine etki eden dinamik bölgesel yüklerin ölçümü üzerine yapılmıştır.

Bu telemetri sistemi ile alınan bölgesel veriler mekanik tasarımcıya tasarımlarını daha dayanımlı, ekonomik ve hafif yapmasına yardım edebilir.

Bu telemetri sistemi iki parçadan oluşmaktadır. Birisi, ölçüm ve veri aktarım devresi diğeri ise alıcı devresidir. Ölçüm devresinin üzerinde dört adet yarım köprü strengaç girişi, ortasında bir adet ivmeölçer ve veri iletişimi için bir alıcı-verici devresi bulunmaktadır. Ölçüm devresi uzama ölçümleri için bir adet enstrümantasyon yükselteci içermektedir. Bu devrede, dijital potansiyometreler otomatik kalibrasyon, sıfırlama ayarları ve kazanç seçimi için kullanılmaktadır. Dijital anahtarlar ise strengaç seçimi için kullanılmaktadır.

Devreler Proteus'ta tasarlanmıştır. PIC mikrokontrolcünün yazılımları HITECH C kullanılarak yazılmıştır ve kullanıcı arayüzü Microsoft Visual Studio kullanılarak oluşturulmuştur.

Sistem çekme basma test cihazı kullanılarak test ve kalibre edilmiştir. Sonrasında, telemetri sistemi bir güneş enerjili yarış aracının -Dokuz Eylül Üniversitesi Solaris- üzerinde gerçek yol koşullarında test edilmiştir.

Anahtar kelimeler: Telemetri, uzama ölçümü, datalogger

CONTENTS

	Pages
M.Sc THESIS EXAMINATION RESULT FORM.....	ii
ACKNOWLEDGEMENTS	iii
ABSTRACT	iv
ÖZ	v
LIST OF FIGURES	viii
LIST OF TABLES	x
CHAPTER ONE - INTRODUCTION	1
1.1 Researches on Telemetry Systems	1
1.2 Aim of the Project	3
1.3 Parts of the Project	3
CHAPTER TWO - METHODOLOGY	4
2.1 Wireless Communication	4
2.2 I ² C and SPI Communication	5
2.3 Strain Measurement.....	7
2.4 System Model of Vehicle	8
2.5 Instrumentation Amplifier	10
CHAPTER THREE - HARDWARE DESIGN	12
3.1 General Overview of the Hardware.....	12
3.2 Calculation of Hardware Requirements for the Project	13
3.3 Microcontroller PIC18F45K22	14
3.4 Accelerometer	15
3.5 RF Transceiver	16
3.6 Instrumentation Amplifier	17

3.7	Strain Gauges	18
3.8	Analog Switches.....	21
3.9	Digital Potentiometers	22
3.10	Specifications of the Telemetry Circuit.....	23
CHAPTER FOUR - SOFTWARE OF THE TELEMETRY SYSTEM.....		25
4.1	Microcontroller Software	25
4.2	Graphical User Interface.....	26
CHAPTER FIVE - EXPERIMENTS AND RESULTS		27
5.1	Tests on the Universal Testing Machine	27
5.2	Tests on the Vehicle Rim	35
CHAPTER SIX - CONCLUSION		39
REFERENCES		40
APPENDICES		43

LIST OF FIGURES

	Pages
Figure 2.1 FSK modulation example	4
Figure 2.2 Channel overlapping at air data rate of 2Mbps.....	5
Figure 2.3 I ² C protocol bus configuration	5
Figure 2.4 SPI protocol bus configuration	6
Figure 2.5 SPI communication data transfer diagram.....	7
Figure 2.6 A linear strain gauge	7
Figure 2.7 System representation of a 1/4 vehicle	9
Figure 2.8 Schematic of instrumentation amplifier.....	11
Figure 3.1 Block scheme of the telemetry circuit	12
Figure 3.2 Pin layout of microcontroller.....	15
Figure 3.3 Block diagram of the MMA8653	16
Figure 3.4 Schematic circuit of the accelerometer.....	16
Figure 3.5 NRF24L01 in the circuit schematic	17
Figure 3.6 Schematic of the instrumentation amplifier and reference input circuit... 18	18
Figure 3.7 Circuit scheme of quarter bridge type-II	19
Figure 3.8 Installation form of quarter bridge type-II.....	19
Figure 3.9 Strain gauge inputs	20
Figure 3.10 Analog switch for powering up strain gauges	21
Figure 3.11 Analog switches for connecting strain gauges to instrumentation amplifier	22
Figure 3.12 Connections of digital potentiometers	23
Figure 3.13 Produced telemetry circuit.....	24
Figure 4.1 Flowchart of the telemetry circuit software.....	25
Figure 4.2 GUI that is developed in the research.....	26
Figure 5.1 Universal testing machine and telemetry setup	28
Figure 5.2 Strain – Time graph obtained using video extensometer	28
Figure 5.3 Results of experiment 1 with designed telemetry system.....	29
Figure 5.4 Results of experiment 2 with designed telemetry system.....	29
Figure 5.5 Digital values of ADC in experiment 3	30

Figure 5.6 Digital values of ADC in experiment 4	30
Figure 5.7 Digital values of ADC in experiment 5	31
Figure 5.8 Load-Strain line from arithmetic mean points.....	31
Figure 5.9 Comparison of experiment 1 values	32
Figure 5.10 Comparison of experiment 2 values	32
Figure 5.11 Comparison of experiment 3 values	32
Figure 5.12 Comparison of experiment 4 values	33
Figure 5.13 Comparison of experiment 5 values	33
Figure 5.14 Result of experiment 1 with data logger.....	34
Figure 5.15 Result of experiment 2 with data logger.....	34
Figure 5.16 Result of experiment 1 with telemetry system	35
Figure 5.17 Result of experiment 2 with telemetry system	35
Figure 5.18 Quarter bridge type-II installation of strain gauges.....	36
Figure 5.19 Installation of the transmitter circuit on the rim	36
Figure 5.20 Telemetry circuit and the rim is attached on the vehicle	36
Figure 5.21 Strain data from the first experiment on the car	37
Figure 5.22 Strain data from the second experiment on the car.....	37
Figure 5.23 Phase difference between strain data.....	38

LIST OF TABLES

	Pages
Table 3.1 Standard data packet of RF transceiver NRF24L01+	17



CHAPTER ONE

INTRODUCTION

1.1 Researches on Telemetry Systems

Rim is one of the most critical parts of automobile when human safety is considered. Rims have important effect on fuel consumption as well. In the development process, car rims are tested on simulation devices. In the simulation, strain values that are measured from critical points of the rim are recorded then these values are evaluated for learning the fatigue characteristics of the rim material. On the simulation devices the sensors should be placed on the turning rim (MTS, 2014). On the other hand, reliability of the simulation is based on the knowledge of the real road conditions where the rim is normally used. At this point, the road profile and the strain data that is taken from the rims of a moving car on a real road are important to use it in laboratory simulation test and to test the sample rim in the real road conditions. Nevertheless, realizing this with a wired measuring system makes the required mechanical systems complex and increases the number of parts those have to be mounted on the vehicle. So, measured strain and acceleration data from a moving car's rim or from a turning test rim in laboratory conditions, should be transmitted to a logger computer with a simple and compact wireless communication device. For the same purpose, Murakami, Morita and Mineki (1997) developed a strain history recorder which was based on rainflow method that records the measured strains on the car rim in a memory card. Murakami, Mineki, Wakamatsu and Morita (1999) used laboratory tests and data acquisition from 3 different types of road in the design process of car rim. In a research (Pytka et al., 2011) rotating wheel dynamometer that logs the measured quantities were used on an off-road vehicle. The dynamometer was placed on the rim without making any change on the vehicle. Another example for instrumented vehicles is given by Blaisdell (1983). The instrumented vehicle contained strain gage torque sensor mounted on the shaft to measure torque on the shaft and three complete strain gage wheatstone bridges on the wheels to measure the loads acting on the vehicle wheel in three directions. In the design process of automobile parts, real world tests are as important as calculations.

Thomas et al. (1999) used user profiles fatigue design process. Doherty (2009) developed and tested an electronic strain gage instrumentation system to understand the real world suspension loads on a racing vehicle. A railway bridge was instrumented with strain transducers and accelerometer to monitor the weights of trains passing and the dynamic effects of them (Karoumi et al., 2005). Another usage of strain gauge on railroad was measuring the contact point between the rail and wheel (Kanehara & Fujioka, 2002). Vehicle tires can be instrumented to give information to the control systems of the vehicle. In the research of Erdogan et al. (2010) vehicle tires were equipped with accelerometers and used as the input for lateral stability control system (ESP). Kuchler (1999) designed a wheel force measuring hub assembly that has strain gauge sensors with slip ring system that uses infrared optical couple communication. In a research (Gutierrez-Lopez et al., 2015) strain measurements of a rim were taken with wired data loggers to verify the results of the simulations. Tests of the rim were performed using a test workbench that can apply force to the rim in single direction. The measurement techniques of strain gauges are given in the research Kester (2005). Strain gauges are connected in Wheatstone bridge form. The output of strain gauge bridge is amplified using instrumentation amplifiers. AD623 (Analog Devices, 2008) instrumentation amplifier that has electronically selectable gain and offset voltage was used on a wireless strain sensor (Nagayama et al., 2004). Instrumentation amplifier amplifies the noise signals, too. Low pass filters are used for reducing the power of noise that is amplified by instrumentation amplifier.

At the beginning of a measurement shunt resistors are used for zeroing the output of the Wheatstone bridge. Strain gauges are affected by temperature changes. To avoid the resistance changes half or full bridge circuits are used (National Instruments, 2014). Poussier et al. (2005) used temperature sensors for obtaining correction graphs for strain gauge measurements. The best result was obtained when Newton interpolation technique was used. Arms et al. (2004) placed their measurement system inside a temperature controllable space to examine the response of the system to the temperature changes.

Lee et al. (2007) compared four different types of wireless communication protocols (Bluetooth, Ultra Wide Band, ZigBee and WiFi) in terms of their data rate, transmission efficiency, power consumption, maximum packet lengths and so on. To increase the reliability of the wirelessly received data packets, packet control bytes should be added to the packet when transmitting (Arms et al., 2004).

1.2 Aim of the Project

In this project, a telemetry system is designed for measuring the local dynamical forces acting on a solar race car. The telemetry circuit is designed especially considering the forces acting on the rim. But the circuit is suitable to measure the strains acting on other critical points on the solar car. The rim is a critical part for safety and a heavy part for a solar race car. The measurements that are taken by the telemetry can be used as a feedback for the design process of the rims. Similarly, measurements can be used to analyze dynamical real road forces acting on any part of the solar car and this will also help the designer to make stronger and lighter designs.

1.3 Parts of the Project

The telemetry system has three parts. These are measurement circuit part which measures the strains and accelerations and transmits the measurements, receiver circuit part which receives the information from the measurement circuit and sends them to a logger computer and graphical user interface part which shows the last measurements to the user and logs them inside the computer.

The works done in the project includes hardware and microcontroller software designs of the measurement circuit and receiver circuit and software of the graphical user interface.

CHAPTER TWO METHODOLOGY

2.1 Wireless Communication

Wireless communication is the data transfer between two or more devices without conductors. Wireless communication can be acquired using optic, sound, radio waves, etc. In this project radio frequency (RF) communication is used. The RF communication module that is used in the project is "NRF24L01+" which uses the industrial scientific medical (ISM) frequency band of 2.4 GHz as center frequency.

NRF24L01+ module uses Gaussian frequency shift keying (GFSK) modulation which is a type of Gaussian filtered frequency shift keying modulation. Graphs of signal and its FSK modulation is given in Figure 2.1 (Murphy and Slattery, 2005).

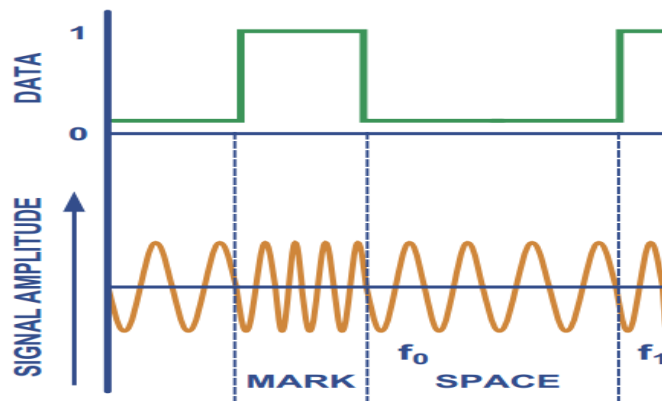


Figure 2.1 FSK modulation example

NRF24L01+ has 3 selectable air data rate which are 250kbps/s, 1Mbps/s and 2Mbps/s. The module has 126 RF channels for 250kbps and 1Mbps. When the module is used at air data rate of 2Mbps only 63 of these channels can be used without channel overlapping. Because the channels have bandwidth of 1MHz but with air data rate of 2Mbps signal occupies 2MHz of bandwidth. Channel overlapping is shown in Figure 2.2.

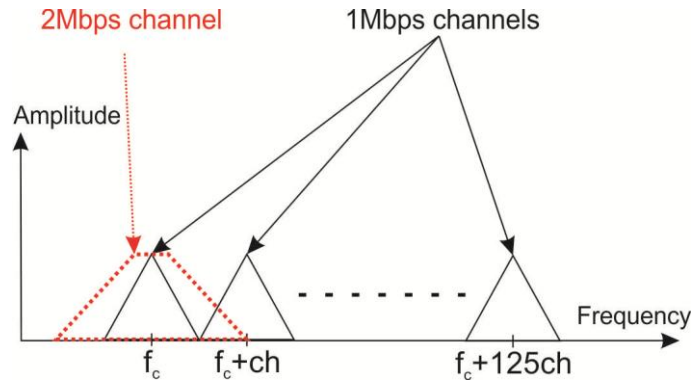


Figure 2.2 Channel overlapping at air data rate of 2Mbps

2.2 I²C and SPI Communication

In this project, two types of wired communication protocols are used. Inter-Integrated Circuit (I²C) is used for accelerometer and Serial Peripheral Interface (SPI) is used for RF module NRF24L01+ and for digital potentiometers.

There are two types of units in I²C protocol one of them is master unit and there is only one master in a I²C bus. Other unit in the I²C protocol is slave unit and the maximum number of slave units is determined by the input and output impedances of the units on the bus.

I²C protocol uses two wire communication. These are serial data line (SDA) and serial clock line (SCL). SDA line is used both for transmitting and receiving the serial data. SCL line determines when the serial data should be taken by the slave unit and the clock signal on the SCL line is generated by the master unit.

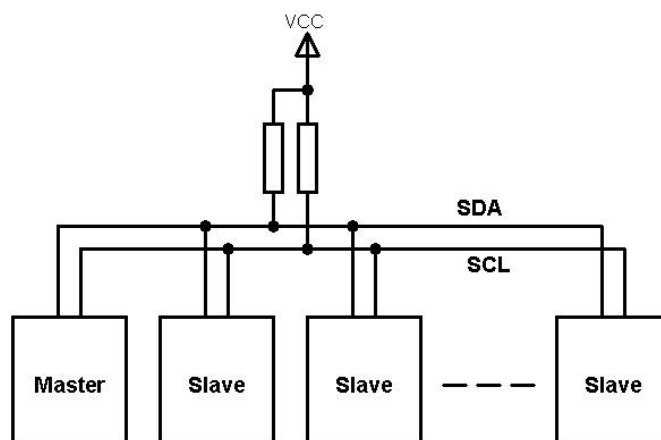


Figure 2.3 I²C protocol bus configuration

Bus configuration of I²C protocol is given in Figure 2.3. It can be seen on the figure that there are pull up resistors connected on the lines SDA and SCL, these pull up resistors are needed in I²C protocol.

SPI protocol uses three wire communication which gives the protocol the ability of full-duplex communication. The wires of SPI protocol are serial clock (SCK), serial data in (SDI) and serial data out (SDO). SDI and SDO lines should be crossed between master and slave units. In some ICs these pins are labeled as master in slave out (MISO) and master out slave in (MOSI). When used in this form the pins don't need to be crossed as the label names determine where the line to be connected both on master and slave. Bus configuration of SPI protocol is given in Figure 2.4. There is one additional pin on each slave unit which is called slave select (SS) in the figure they are low active. SS pin is used to select the slave unit to communicate. This pin is input for slave units and output for master unit.

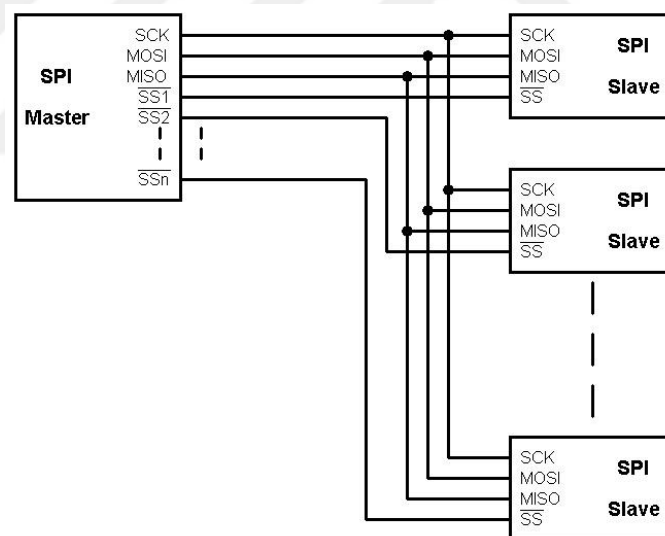


Figure 2.4 SPI protocol bus configuration

There are one shift register and a buffer for SPI communication. Serial buffer sends the data to be transmitted to the shift register and gets the received data from the shift register by parallel communication. Shift register is used both for transmitting and receiving the serial data. By every single cycle of the serial clock signal shift register sends out and gets in one bit of information. In Figure 2.5 data transfer diagram is shown.

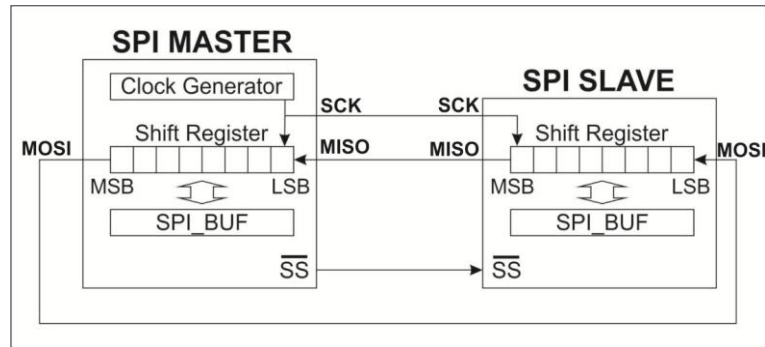


Figure 2.5 SPI communication data transfer diagram

2.3 Strain Measurement

In this project, strain measurements on mechanical samples are taken using strain gauges. Strain gauges are devices that their resistance changes with the forces acting on them. Force that acts on the strain gauge changes the length of it. Strain gauges have resistive materials which is placed in such a way that when a force is applied the resistive material's size changes. Form of a linear strain gauge is given in Figure 2.6.

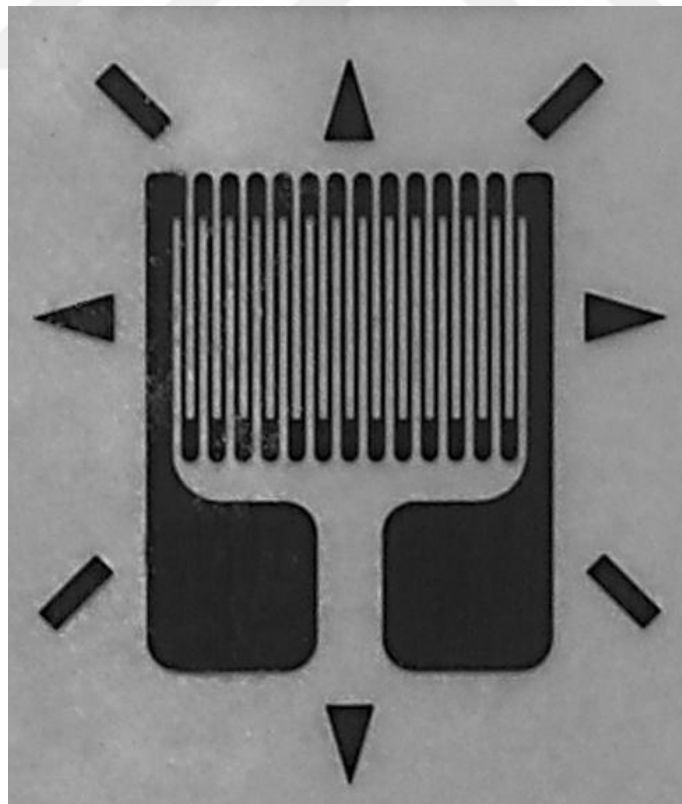


Figure 2.6 A linear strain gauge

When a force acts on the strain gauge in vertical direction according to the paper, it can be seen that there are $n=26$ resistive column inside the example strain gauge which their size change.

$$R = \rho \frac{l}{A} \quad (2.1)$$

Basic resistance formula is given in Eq. (2.1). Where R is resistance, ρ is resistivity, l is length and A is the cross-sectional area of the material. Considering the strain gauge in Figure 2.6 when there is a vertical strain of l total elongation of the material is $n \cdot l = 26l$. So the resistance change is more sensitive to the strain due to the number of columns in the strain gauge.

Gauge factor is the property of strain gauge and it's formula is given in Eq. (2.2). GF is the gauge factor, ΔR is the change in resistance due to Δl (change in length) and ϵ is called strain.

$$GF = \frac{\Delta R}{R} \frac{\Delta l}{l} = \frac{\Delta R}{R \epsilon} \quad (2.2)$$

2.4 System Model of Vehicle

A wheel of a vehicle can be represented as two mass-spring-damper system as shown in Figure 2.7. One of them is the suspension and the other is the tire.

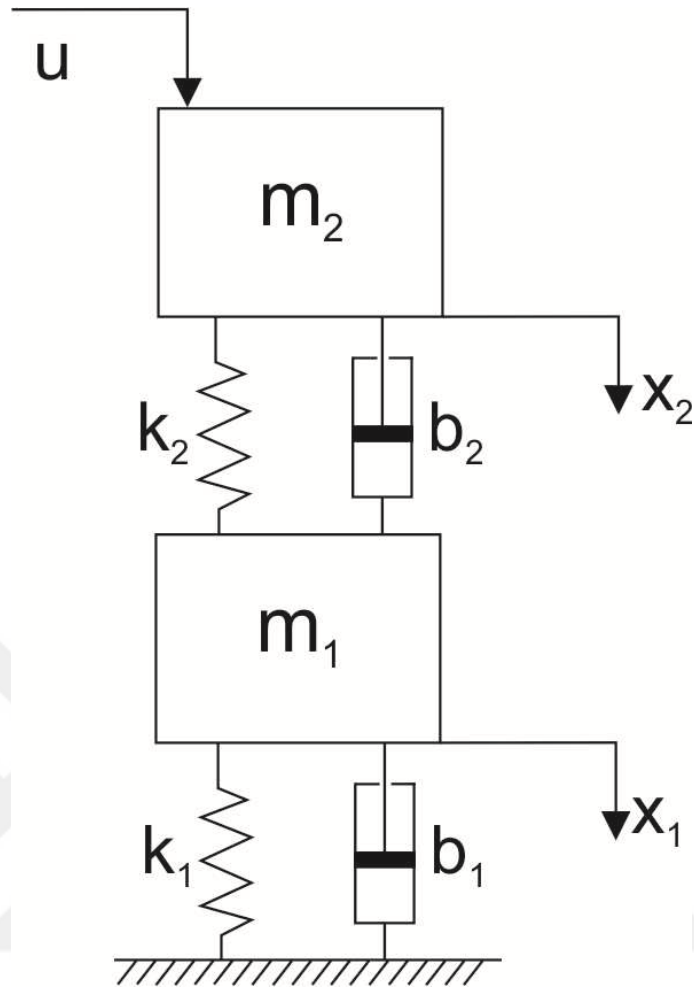


Figure 2.7 System representation of a 1/4 vehicle

m_1 : Mass of tire

k_1 : Spring constant of tire

b_1 : Damper constant of tire

m_2 : 1/4 mass of vehicle and suspension

k_2 : Spring constant of suspension

b_2 : Damper constant of suspension

x_1 : Displacement of center of gravity of wheel

x_2 : Displacement of connection point of suspension with the vehicle

u : External force

The governing equations of motion are given as;

$$m_1 \ddot{x}_1 = -k_1 x_1 - k_2 (x_1 - x_2) - b_1 \dot{x}_1 - b_2 (\dot{x}_1 - \dot{x}_2) \quad (2.3)$$

$$m_2 \ddot{x}_2 = -k_2(x_2 - x_1) - b_2(\dot{x}_2 - \dot{x}_1) + u \quad (2.4)$$

By taking the Laplace transforms of these equations transfer functions of displacements are given below.

$$\frac{X_1(s)}{U(s)} = \frac{b_2 s + k_2}{[m_1 s^2 + (b_1 + b_2)s + k_1 + k_2][m_2 s^2 + b_2 s + k_2] - (b_2 s + k_2)^2} \quad (2.5)$$

$$\frac{X_2(s)}{U(s)} = \frac{m_1 s^2 + (b_1 + b_2)s + (k_1 + k_2)}{[m_1 s^2 + (b_1 + b_2)s + k_1 + k_2][m_2 s^2 + b_2 s + k_2] - (b_2 s + k_2)^2} \quad (2.6)$$

2.5 Instrumentation Amplifier

Instrumentation amplifier is used for amplifying low amplitude signals or low voltage changes. This amplifier type has differential input. Instrumentation amplifier topology is shown in Figure 2.8.

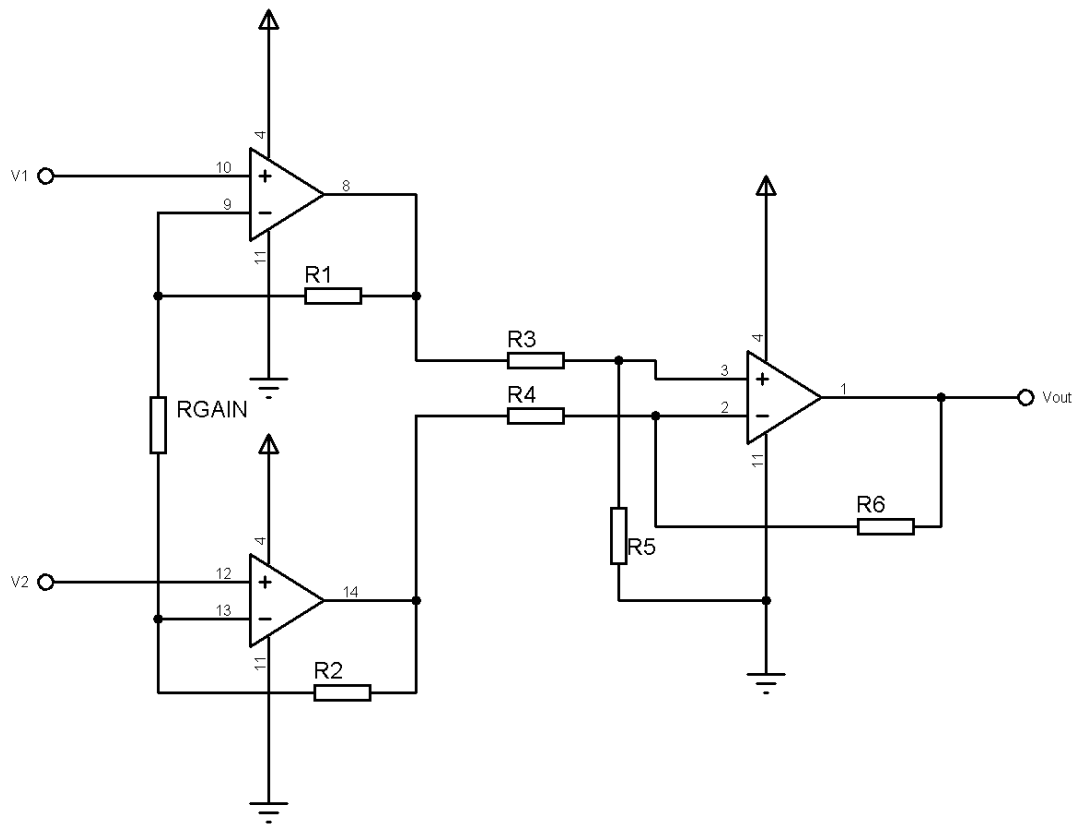


Figure 2.8 Schematic of instrumentation amplifier

In this research instrumentation amplifier is used for amplifying the signal of the strain gage quarter bridge type II.

Output of the instrumentation amplifier is

$$V_{out} = \frac{R_6}{R_4} \left(1 + \frac{2R_5}{R_G} \right) (V_1 - V_2) \quad (2.7)$$

CHAPTER THREE HARDWARE DESIGN

3.1 General Overview of the Hardware

The telemetry circuit is designed with four quarter bridge type-II strain gauge inputs and an accelerometer. There is instrumentation amplifier on the circuit to amplify the signals of the strain gauges. Digital potentiometers are used to calibrate strain gauges, to set the gain of the instrumentation amplifier, to set the offset of the instrumentation amplifier. As the circuit is designed for taking measurements from rotating specimens, circuit should have been designed with low power consumption. To accomplish this purpose the strain gauges are activated only when they are being measured because they have the lowest impedance among other components of the circuit. Block scheme of the telemetry circuit is shown in Figure 3.1.

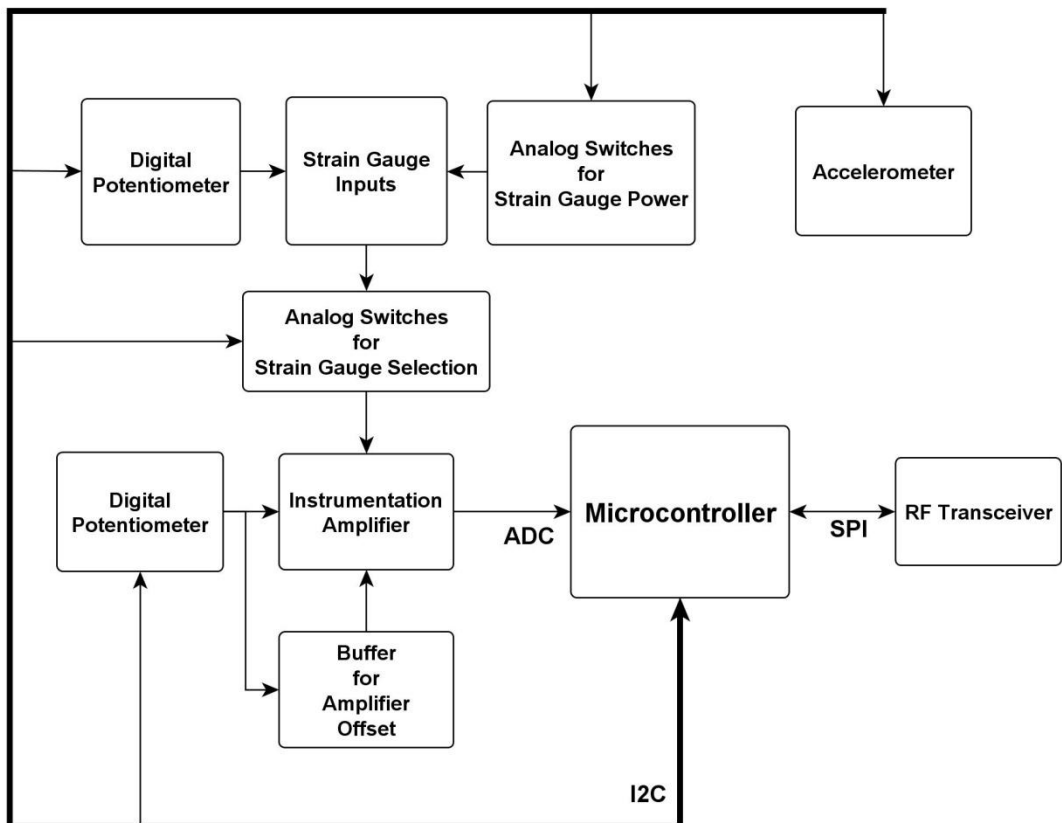


Figure 3.1 Block scheme of the telemetry circuit

Analog switches are used for powering up strain gauges and selecting only one of the strain gauge bridge output for instrumentation amplifier's input. By using analog switches only one instrumentation amplifier is used for four strain gauge bridges.

Microcontroller is used for communicating with accelerometer, analog switches, digital potentiometers via I²C and RF transceiver via SPI. One of Analog to Digital Converter (ADC) input of microcontroller is used for measuring the output of the instrumentation amplifier.

In this chapter, transmitter circuit of the telemetry system is represented. The receiver circuit's schematic and PCB layout is given in appendix.

3.2 Calculation of Hardware Requirements for the Project

The telemetry circuit is designed considering the system will measure strain data from a moving car with the speed of 120 km/h.

For a car which has wheel diameter of 0.64m, angular velocity of the wheel will be;

$$\frac{120 \left[\frac{km}{h} \right] * 1000 \left[\frac{m}{km} \right]}{3600 \left[\frac{s}{h} \right] * 0,64[m] * \pi} = 16.58[RPS] \quad (3.1)$$

In Eq. (3.1) angular velocity is given, for this velocity there is 15.1 ms of duration for measuring four strain gauges, reading an accelerometer and transmitting these measurements.

The time needed for reading accelerometer data ($t_{accelerometer}$) through I²C with 1MHz module frequency is calculated below. There are three 10 bit accelerometer data which each of them are held in two 8 bit registers and 8 bit preamble.

$$t_{accelerometer} = (16x3 + 8) \frac{1}{10^6} = 56\mu s \quad (3.2)$$

There are four strain gauges to be measured using ADC of the microcontroller. For each of the strain gauges instrumentation amplifier will need a settling time (t_{amp_set}) which is equal to a maximum of $350\mu s$. In equation (3.3) t_{c_adc} which is the time needed for the capacitor of the ADC to be charged is equal to $1.2\mu s$, t_{AD} is ADC standby time before starting conversion and equal to 16 ADC clock which is $16\mu s$. ADC conversion time (t_{conv}) is equal to $10\mu s$ because it is used in 10bit mode.

$$t_{gauge} = 4(t_{amp_set} + t_{c_adc} + t_{AD} + t_{conv}) = 1508.8\mu s \quad (3.3)$$

There will be a time ($t_{transmit}$) needed to transfer these measurements. RF transceiver module has a time before changing its mode to transmit (TX) mode it is called TX settling time ($t_{tx_settling}=130\mu s$). After changing the mode the data will be send with the speed of 2Mbps, time needed for this is called t_{data} . Data packet is given in Table 3.1 which is 97 bit.

$$t_{transmit} = t_{tx_settling} + t_{data} = 178.5\mu s \quad (3.4)$$

Total time needed for measurements and transmitting (t_{total}) is given below.

$$t_{total} = t_{accelerometer} + t_{gauge} + t_{transmit} = 1743.3\mu s \quad (3.5)$$

So the maximum measurement frequency of the telemetry is 573.6 Hz.

3.3 Microcontroller PIC18F45K22

In this project PIC18F45K22 microcontroller is used. Important features of this microcontroller are;

- Up to 64 MHz clock frequency
- 10 bit resolution ADC up to 30 channels
- Fixed Voltage Reference (FVR) for ADC
- Two Master Synchronous Serial Port (MSSP) modules which can be set as I2C or SPI
- 5 Pulse Width Modulation (PWM) outputs

This microcontroller has several package options, in the project 44-pin Thin Quad Flat Pack (TQFP) type of package is selected. Because this package is both small sized and easily soldered by hand. In Figure 3.2 microcontroller part of the schematic of the telemetry circuit is given.

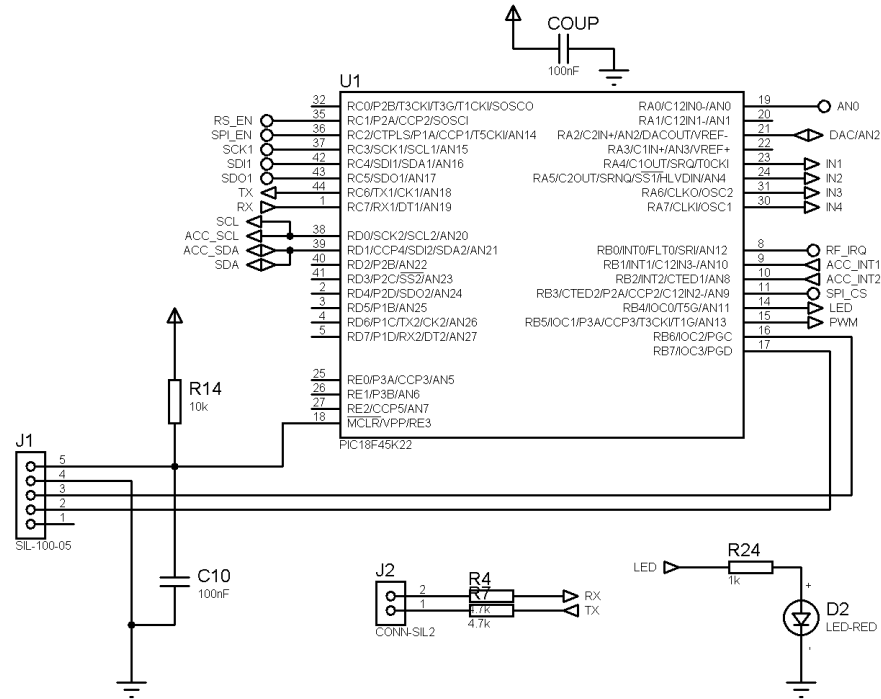


Figure 3.2 Pin layout of microcontroller

First MSSP module is used in SPI mode to communicate with RF module, second MSSP module is used in I²C mode both for digital potentiometers and accelerometer. PIC is programmed using J1 in Figure 3.2, it is called In Circuit Serial Programming (ICSP).

3.4 Accelerometer

In this research MMA8653 3-axis digital accelerometer is used. Accelerometer has digitally selectable scales of $\pm 2g$, $\pm 4g$ and $\pm 8g$. Block diagram of the accelerometer is shown in Figure 3.3 (Freescale Semiconductor 2014). There is Coulomb to Volt (C-to-V) converter inside the IC. The voltage output of the transducers are converted to digital values using embedded ADC which has 10 bit resolution. MMA8653 uses I²C communication. Accelerometer is placed at the middle of the telemetry circuit board. Accelerometer circuit is given in Figure 3.4.

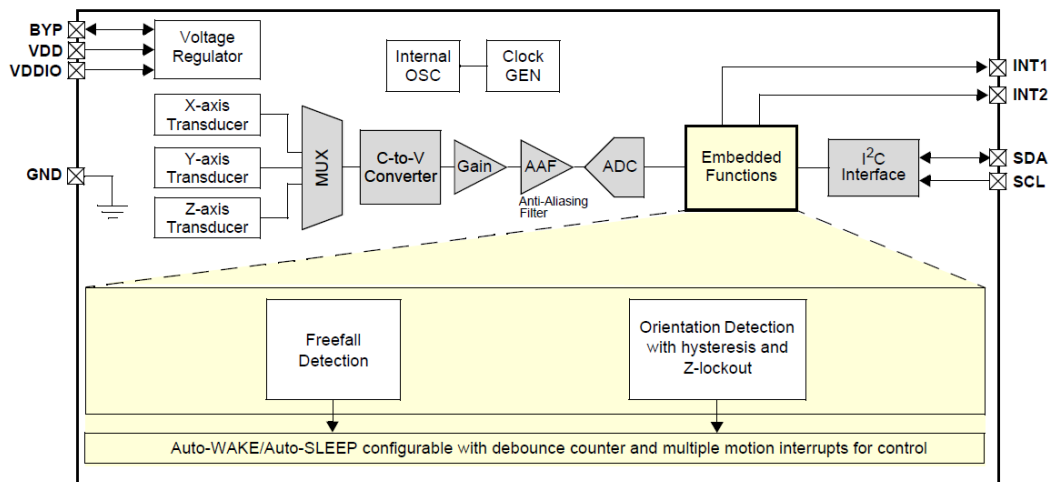


Figure 3.3 Block diagram of the MMA8653

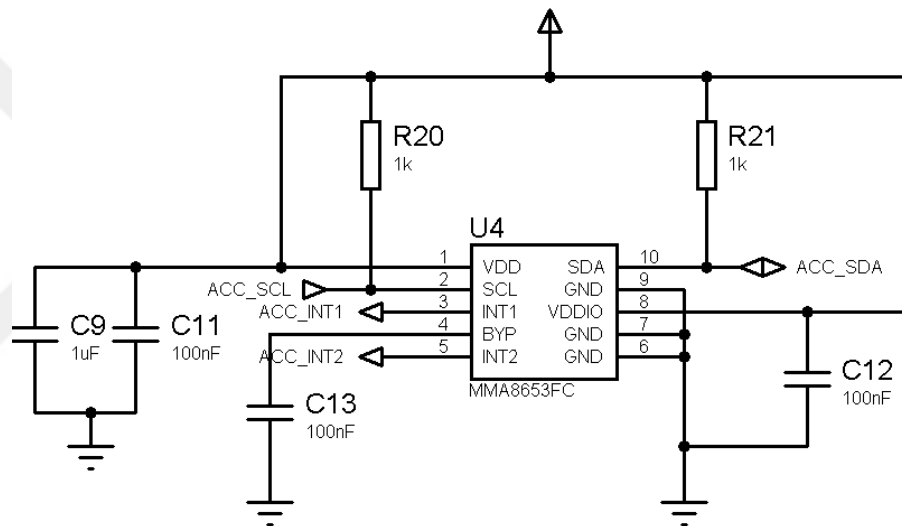


Figure 3.4 Schematic circuit of the accelerometer.

3.5 RF Transceiver

In the research NRF24L01+ RF transceiver module is used. This module has air data rate up to 2Mbps. It uses SPI communication and controlled by build in registers. Module sends and receives data payload of 32 bytes long. Module has auto acknowledgement feature if acknowledgement packet is not received by the transmitting module it automatically retransmits the same data packet.

Table 3.1 Standard data packet of RF transceiver NRF24L01+

Preamble	Address	Packet Control Field	Payload	CRC
1 byte	3-5 byte	9 bit	0-32 byte	1-2 byte

As it is seen in Table 3.1 module uses Cyclic Redundancy Check (CRC) of 1 or 2 bytes. It automatically calculates and checks this field. In Figure 3.5 NRF24L01+ is shown. Module is controlled using SPI communication.

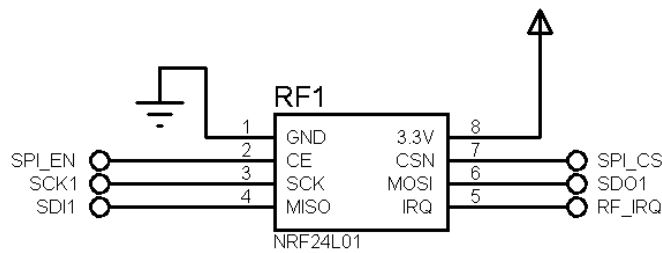


Figure 3.5 NRF24L01 in the circuit schematic

3.6 Instrumentation Amplifier

The instrumentation amplifier that is used in this research is AD8226. This amplifier is chosen because of its low supply voltage, high slew rate, low offset voltage and high gain (Analog Devices, 2012). The amplifier has offset voltage pin which determines the output offset voltage. When both inputs of the instrumentation amplifier is equal output of the instrumentation amplifier is equal to the reference input. Gain selection is accomplished using digital potentiometers. Reference input of the instrumentation amplifier is connected to the output of a buffer which can be controlled using (Digital to Analog Converter) DAC output or PWM output of microcontroller or via voltage divider circuit which is established using digital potentiometers. Schematic circuit of instrumentation amplifier is given in Figure 3.6.

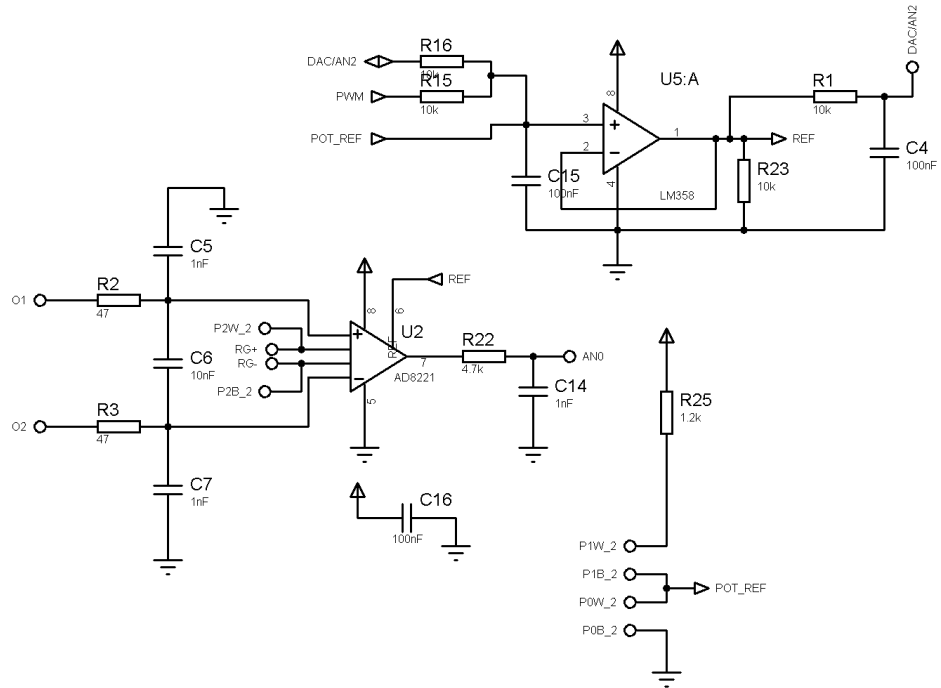


Figure 3.6 Schematic of the instrumentation amplifier and reference input circuit

In Figure 3.6 there can be seen a RC passive low pass filter at the output of the instrumentation amplifier. Low pass filter is calculated considering the fastest measurement cycles.

$$f_{cutoff} = \frac{1}{2\pi RC} = 33,9 \text{ [kHz]} \quad (3.6)$$

The cutoff frequency (f_{cutoff}) of a RC filter is given in equation (3.6). Signals with a higher frequency than the calculated frequency is filtered.

3.7 Strain Gauges

Strain measurements are affected by temperature as they are not taken in laboratory conditions. So strain gauge inputs of circuit were chosen as quarter bridge type-II. The scheme of quarter bridge type-II is given in Figure 3.7 (National Instruments, 2006).

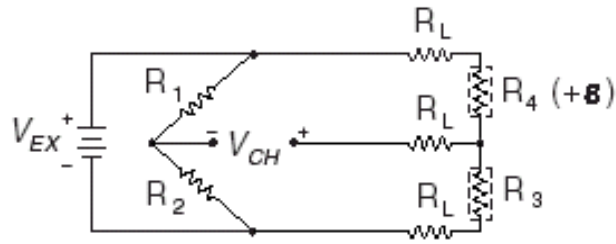


Figure 3.7 Circuit scheme of quarter bridge type-II

R1,R2: Completion resistors of wheatstone bridge on the circuit

R3: Dummy strain gauge that is installed in a way that is not affected by strains

RL: Resistance of the cables that is between the circuit and the strain gauges

R4: Strain gauge that is used for the measurement

The placement of the strain gauges on the specimen is given in Figure 3.8 (National Instruments, 2006). The resistance of R_4 changes with strain and also with the temperature change. To overcome the resistance change that can be occurred by temperature change, dummy strain gauge R_3 is installed in such a way that it is not affected by strain but heat transfer between strain gauge and specimen can be provided.

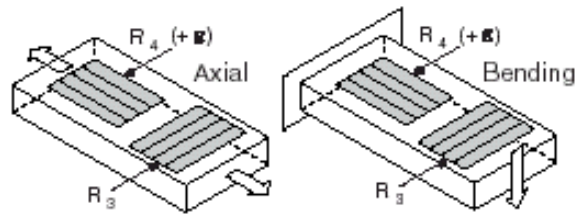


Figure 3.8 Installation form of quarter bridge type-II

Strain gauge bridge circuit's output voltage level is very low for detecting it by the ADC of microcontroller. Instrumentation amplifier is used for amplifying the bridge output to a level that the microcontroller can detect. Microcontroller's ADC has 10 bits resolution this refers to 0.0029V per one bit for 3V of ADC supply voltage. In Figure 3.7, as R_1 and R_2 have the same value $V_{CH(-)}$ will have a potential of $V_{EXT}/2$ [V] referring to negative side of V_{EXT} . Strain gauge's resistance will be changed when its length is changed. Strain gauge's manufacturer supplies the gauge factor (GF) information. The strain gauges that were used in the research have nominal resistance of 350Ω and the gauge factor is 2.155. Using Eq. (2.2), for 0.1%

of enlargement of strain gauge, ΔR is calculated as 0.75425Ω and the new value of the gauge resistance is 350.75425Ω . In this situation, $V_{CH(+)}$ is equal to $0.49946V_{EXT}$. For 10bit of ADC resolution V_{EXT} is equal to 1023 (digital value), $V_{CH(-)}$ is 511.5 and $V_{CH(+)}$ will be 510.94758 (digital value without quantization). Potential difference between $V_{CH(+)}$ and $V_{CH(-)}$ is equal to 0.55242. Output of the bridge will be amplified and for a gain of 1000, the output of the instrumentation amplifier will have a potential of 552.42 (digital value). So, the calibration constant is theoretically calculated in Eq. (3.7). In Figure 3.9 strain gauge bridge circuits and strain gage connectors are shown.

$$1000 [\mu\epsilon] / 552.42 = 1.81 [\mu\epsilon/\text{bit}] \quad (3.7)$$

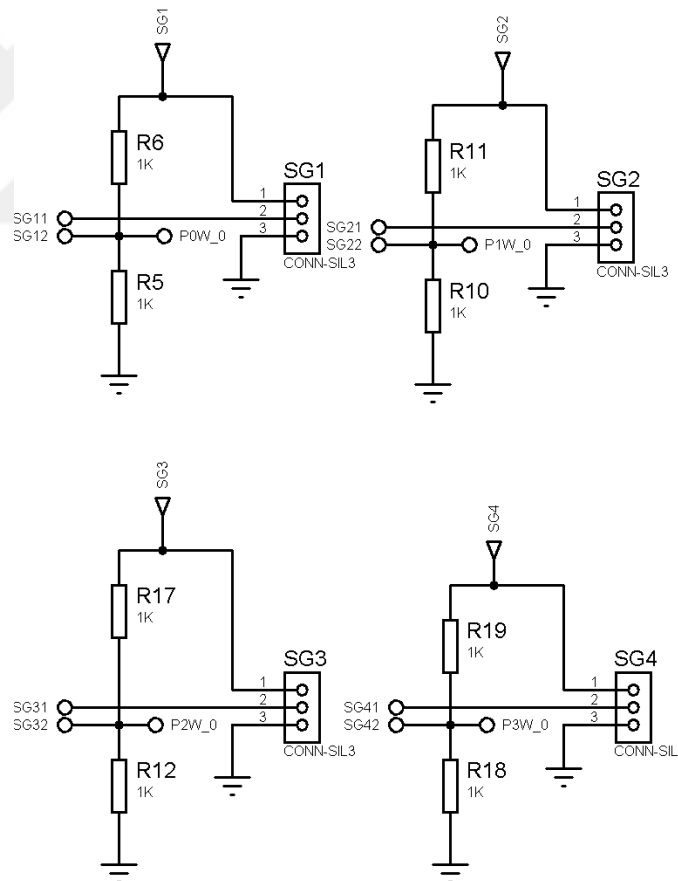


Figure 3.9 Strain gauge inputs

It can be seen that none of the strain gauge bridge circuit is initially powered through voltage supply of the circuit.

3.8 Analog Switches

Analog switches are used in the circuit to power the strain gauges and to connect the selected strain gauge bridge to the instrumentation amplifier. In Figure 3.10 the analog switch IC for powering up the strain gauges is shown.

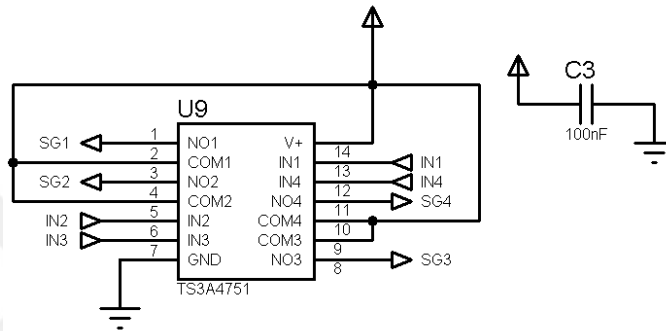


Figure 3.10 Analog switch for powering up strain gauges

Analog switch IC TS3A4751 has 4 Single Pole-Single Throw (SPST) analog switch circuits inside (Texas Instruments, 2006). Analog switches inside the IC has 3 pins which are Input (IN_x), Normally Open (NO_x) and Common (COM_x). All of the common pins are connected to the voltage supply and normally open pins are connected to the strain gauge bridges' supply lines. Input pins are connected to the microcontroller. This gives the circuit the ability to control the power consumption of the strain gauges, because used strain gauges which are 350Ω type have relatively low impedance considering other components of the circuit.

Connection circuit between the instrumentation amplifier and strain gauges is given in Figure 3.11.

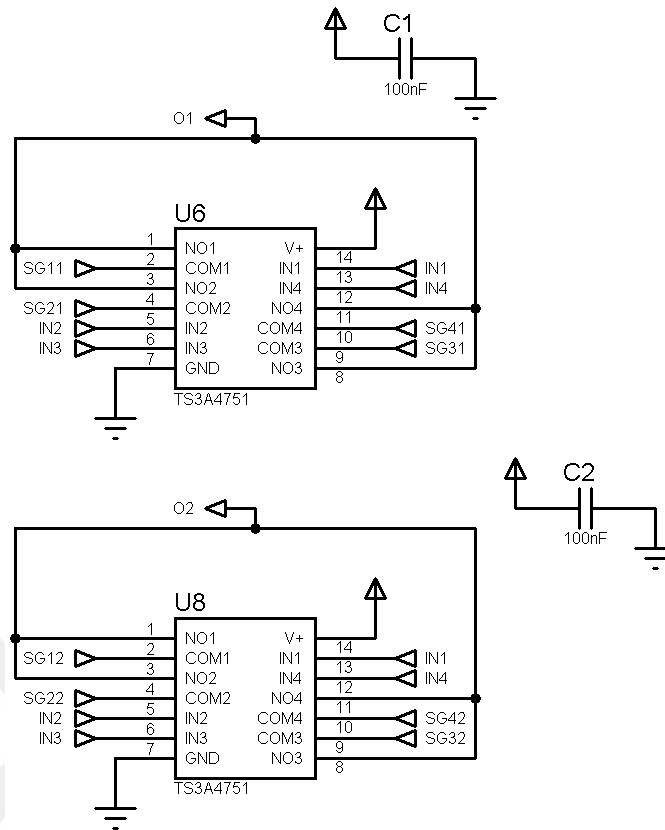


Figure 3.11 Analog switches for connecting strain gauges to instrumentation amplifier

Two analog switch ICs are used for connecting the output of strain gauge bridges' to instrumentation amplifier's input. One of the IC's common pins are connected to the positive input of instrumentation amplifier and the other IC's common pins are connected to the negative input of the instrumentation amplifier. Connections of these ICs are shown in Figure 3.11.

3.9 Digital Potentiometers

Digital potentiometers are used in the circuit for calibrations. These are used in strain gage bridge circuit, to set the gain and the offset of the instrumentation amplifier.

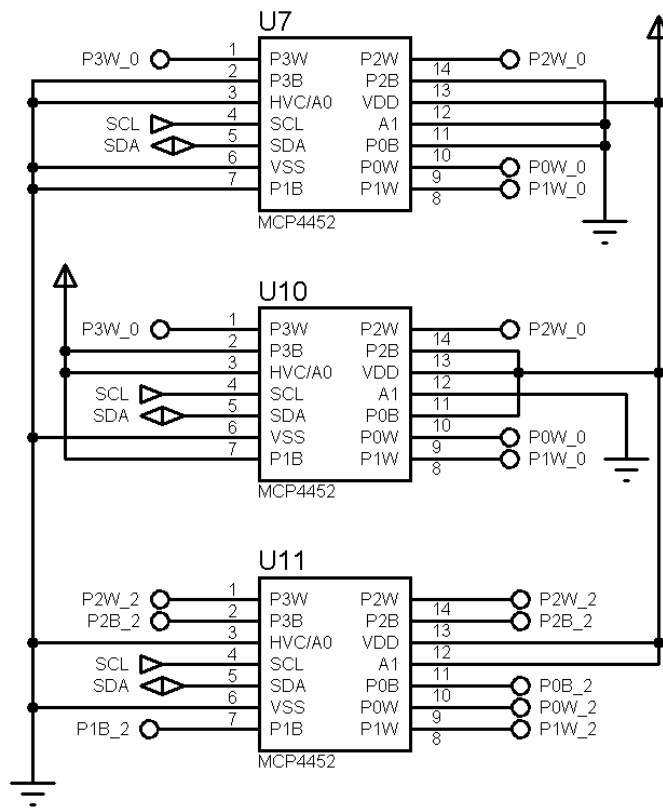


Figure 3.12 Connections of digital potentiometers

There are four variable 2 pin resistors in the IC MCP4452. These digital potentiometer's connections are given in Figure 3.12.

3.10 Specifications of the Telemetry Circuit

The produced telemetry circuit is shown in Figure 3.13. Specifications of the designed strain and acceleration measurement circuit are;

- Total size : 65mm x 35mm x 35mm
- Weight with battery (18650) : 60gr
- 4 quarter/half bridge strain gauge inputs
- Embedded 3-axis accelerometer, $\pm 2g$, $\pm 4g$, $\pm 8g$ selectable acceleration measurement intervals
- On board 2.4 GHz 2Mbit/s RF transceiver

- Packet delivery frequency: 150 packets/sec
- Maximum strain interval: $\pm 50000\mu\epsilon$
- Gain is selectable wirelessly up to 1000
- Accuracy: $\pm 10\mu\epsilon$ @1000 gain
- Resolution: $1.7751\mu\epsilon/\text{bit}$ @1000 gain
- Measurement interval: $\pm 488\mu\epsilon$ @1000 gain

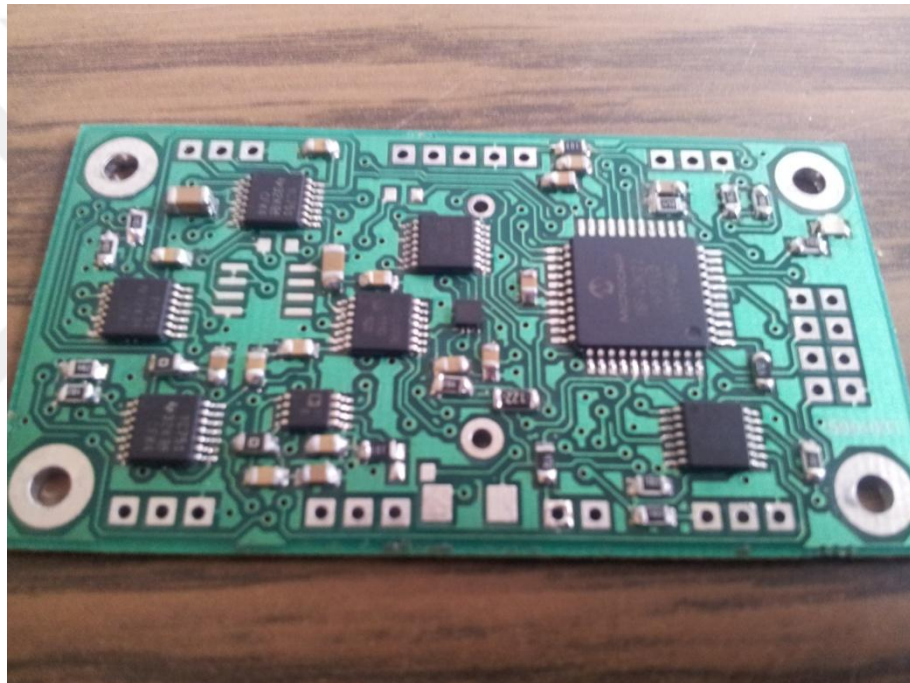


Figure 3.13 Produced telemetry circuit

CHAPTER FOUR

SOFTWARE OF THE TELEMETRY SYSTEM

In the research, software has been developed for microcontroller in MPLAB using HITECH C and Graphical User Interface (GUI) is prepared in Visual Studio using C#.

4.1 Microcontroller Software

Microcontroller software's flowchart is shown in Figure 4.1.

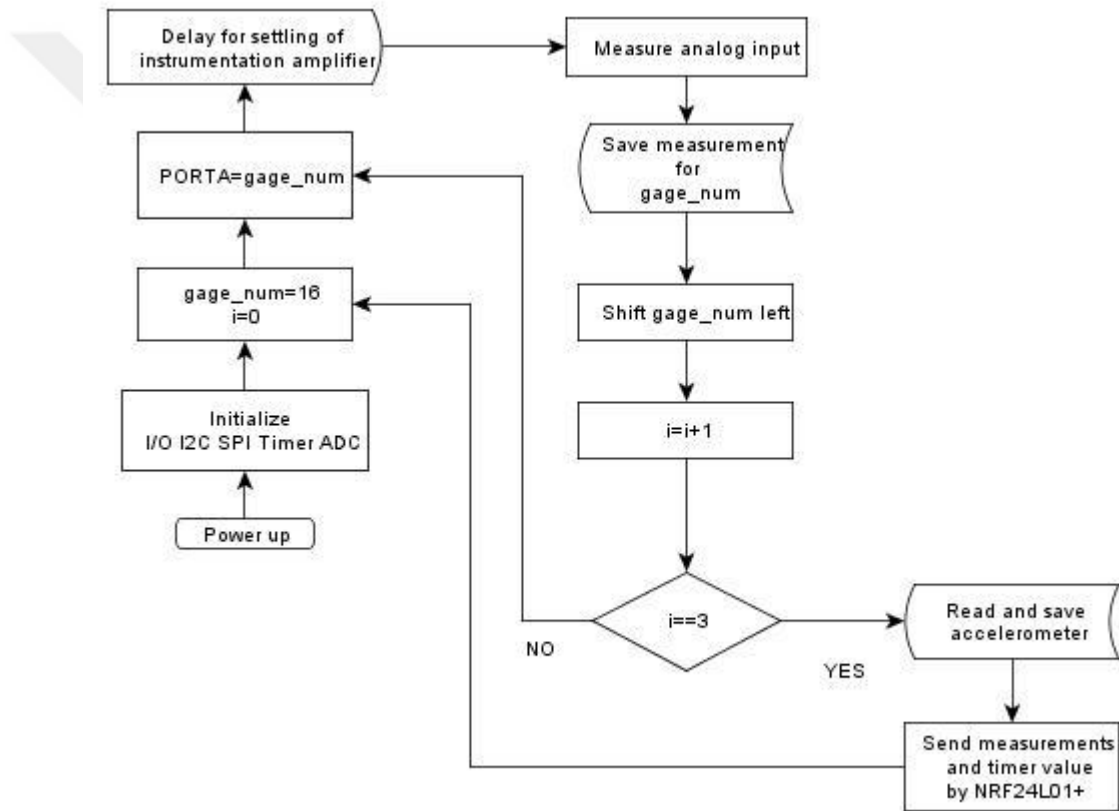


Figure 4.1 Flowchart of the telemetry circuit software

At the first step microcontroller pins are configured as inputs or outputs, I²C, SPI, timer and ADC modules are initialized. Four of the strain gage inputs are measured after that accelerometer is read and all measurements and the value of the timer is sent by NRF24L01+.

4.2 Graphical User Interface

The data that is wirelessly sent from the measurement circuit is sent to the computer by UART (Universal Asynchronous Receiver Transmitter) interface of receiver circuit. In the research a GUI is developed in Visual Studio. In the GUI (Figure 4.2) user is able to observe four strain gauges' and 3-axis accelerometer's data up to four telemetry circuit. GUI also logs the received data to a text file.

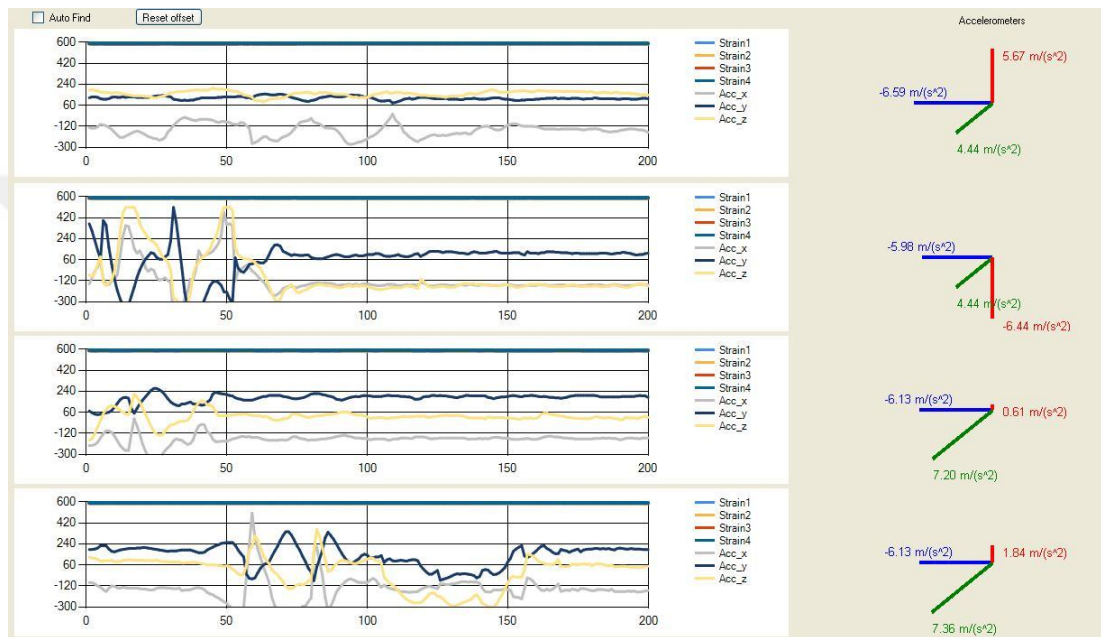


Figure 4.2 GUI that is developed in the research

CHAPTER FIVE

EXPERIMENTS AND RESULTS

In this research the produced telemetry circuit is firstly tested on a universal testing machine, after that circuit is tested on the rim of a electric vehicle car of DEU Solaris solar car team which is being charged using solar charge station of the team.

5.1 Tests on the Universal Testing Machine

In the experiments on the universal testing machine, load was applied to the specimen in predetermined cycles (Figure 5.1). According to the comparison of output of the designed circuit and the laboratory equipments' output, designed telemetry system was calibrated. This calibration was performed to convert the digital output of DAC to real strain unit [$\mu\text{m}/\text{m}$]. The gain of the instrumentation amplifier on the measurement circuit was set to 1000 before starting the measurements. First tests were taken by using video extensometer.



Figure 5.1 Universal testing machine and telemetry setup

In the first experiment, a load that had two periods between 3000 N and 1000 N is applied by the test equipment to the specimen and the load had a rate of 50 N/s. This experiment repeated once more. The result of the first experiment that was taken from the video extensometer is given in Figure 5.2.

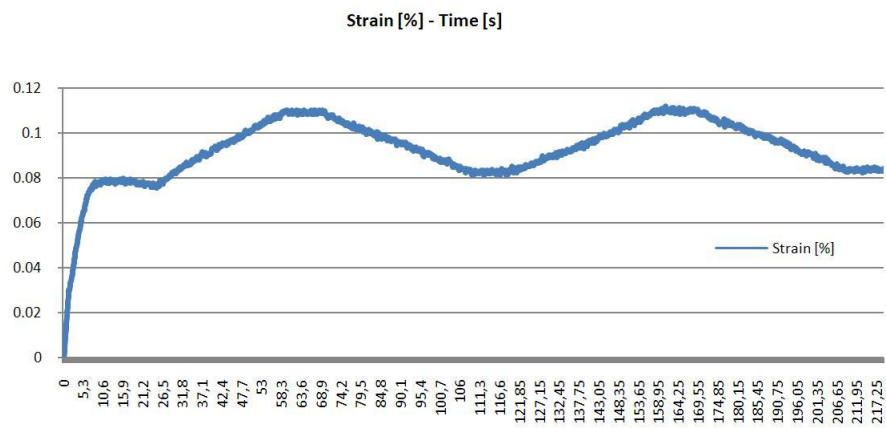


Figure 5.2 Strain – Time graph obtained using video extensometer

In the experiments, measurements were also simultaneously obtained using the telemetry system that had been built. Digital values which were the output of microcontroller's ADC in the experiment 1 and 2 are given in Figure 5.3 and Figure 5.4 respectively. These digital values were used for testing the linearity of the telemetry system.

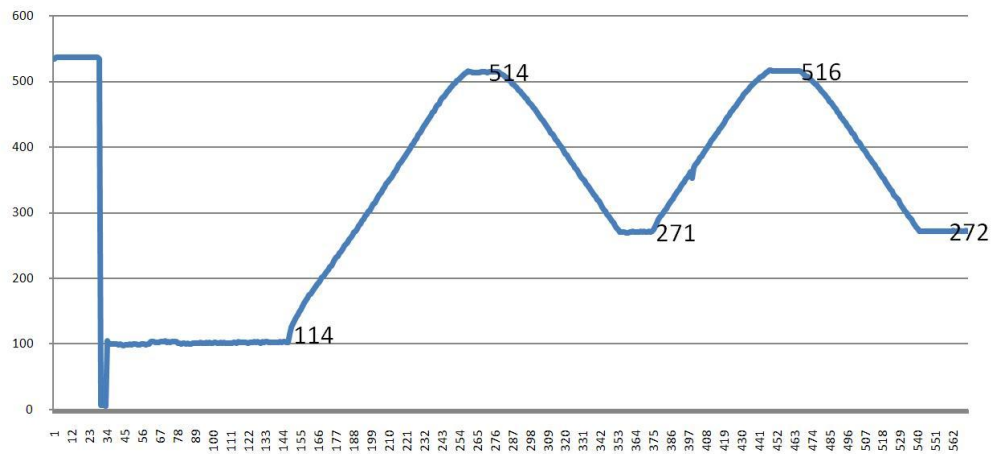


Figure 5.3 Results of experiment 1 with designed telemetry system

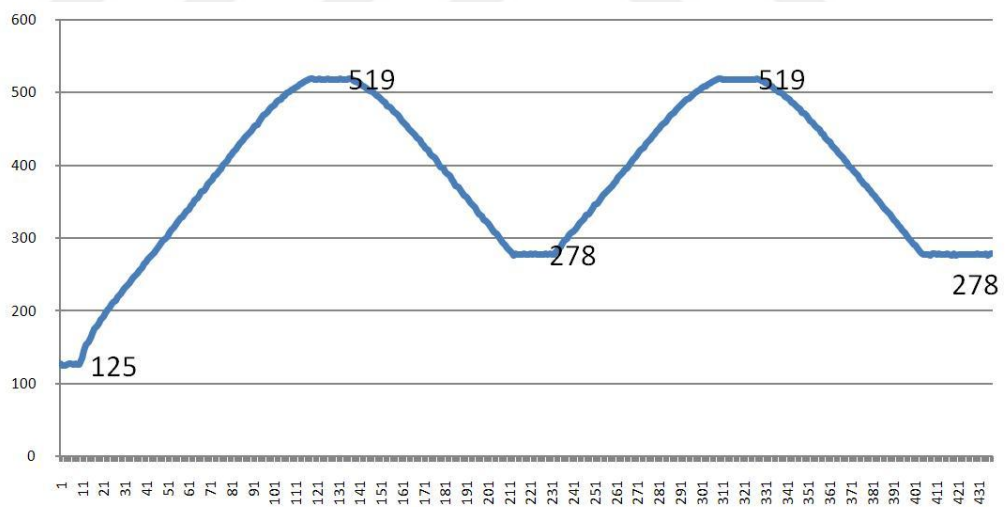


Figure 5.4 Results of experiment 2 with designed telemetry system

In the following experiments universal testing machine was set to two periods between 500 N and 2000 N loads and the rate was set to 25 N/s (Figure 5.5, Figure 5.6 and Figure 5.7).

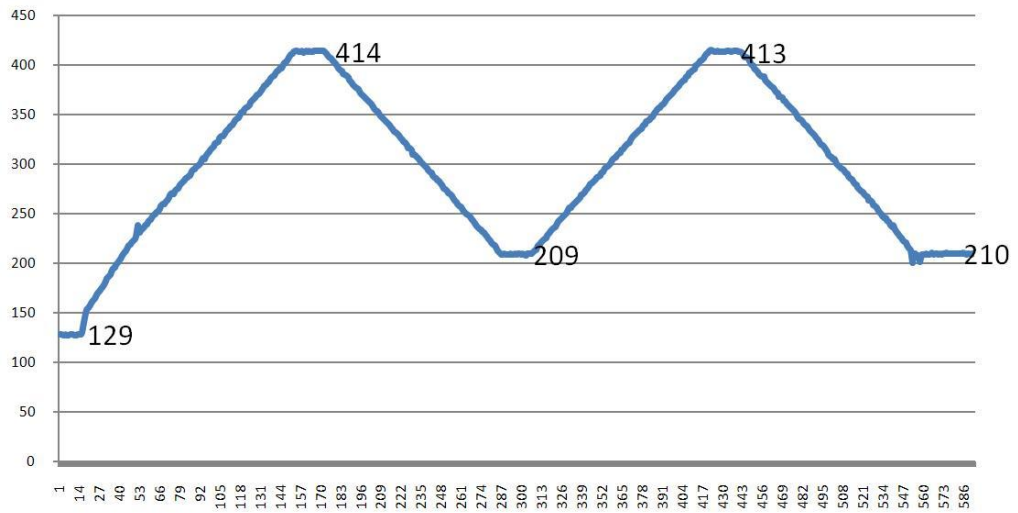


Figure 5.5 Digital values of ADC in experiment 3

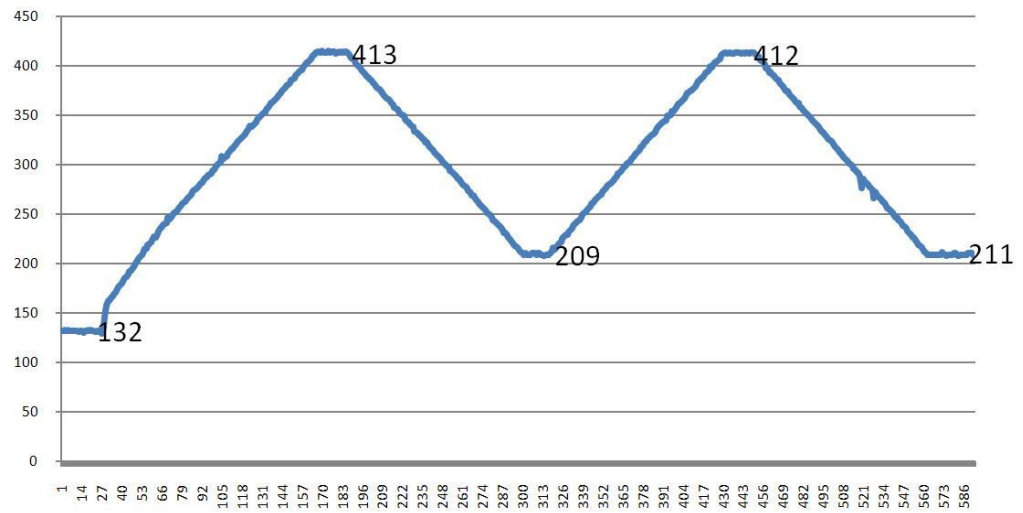


Figure 5.6 Digital values of ADC in experiment 4

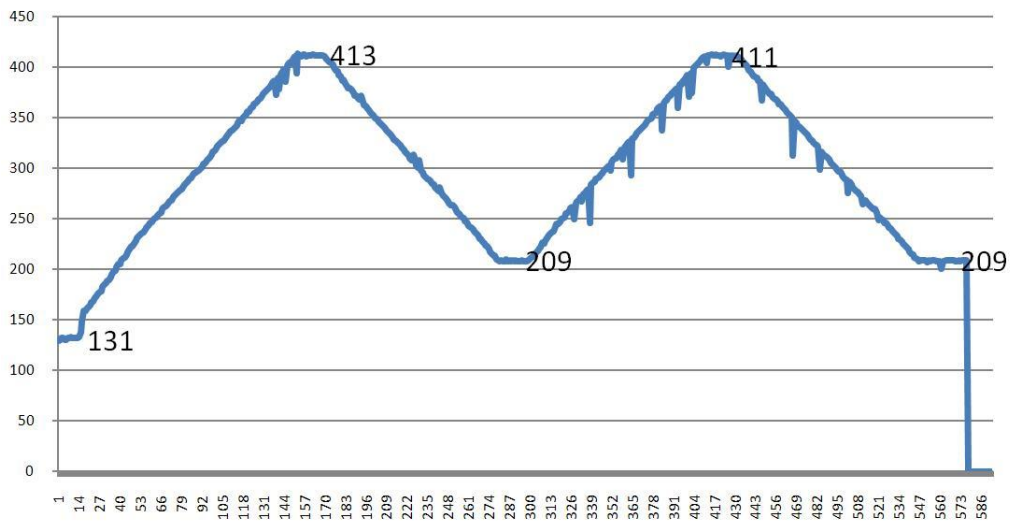


Figure 5.7 Digital values of ADC in experiment 5

From the five graphs of the experiments above, a line equation was obtained by using arithmetic means of two specified points. The graph of the line that was obtained from the arithmetic mean points is given in Figure 5.8.

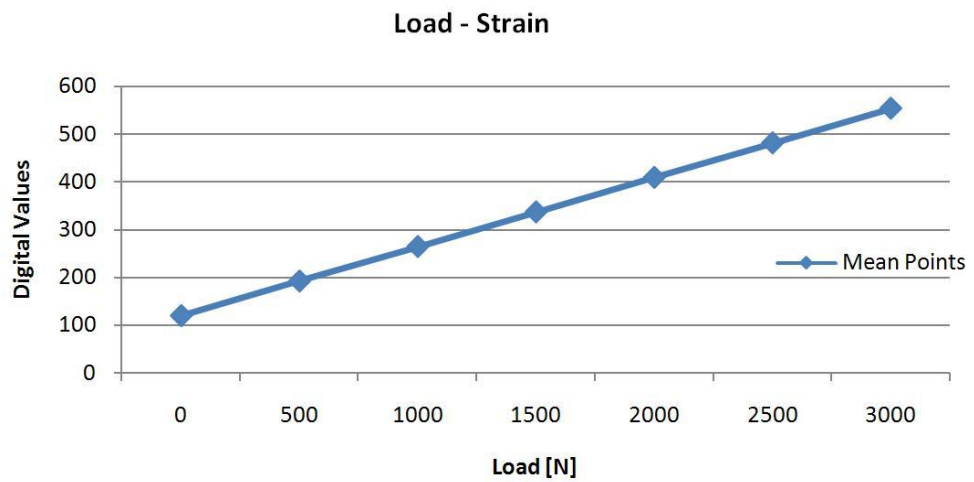


Figure 5.8 Load-Strain line from arithmetic mean points

Results of the experiments were added on the line and the obtained graphs are given in Figure 5.9 - Figure 5.13.

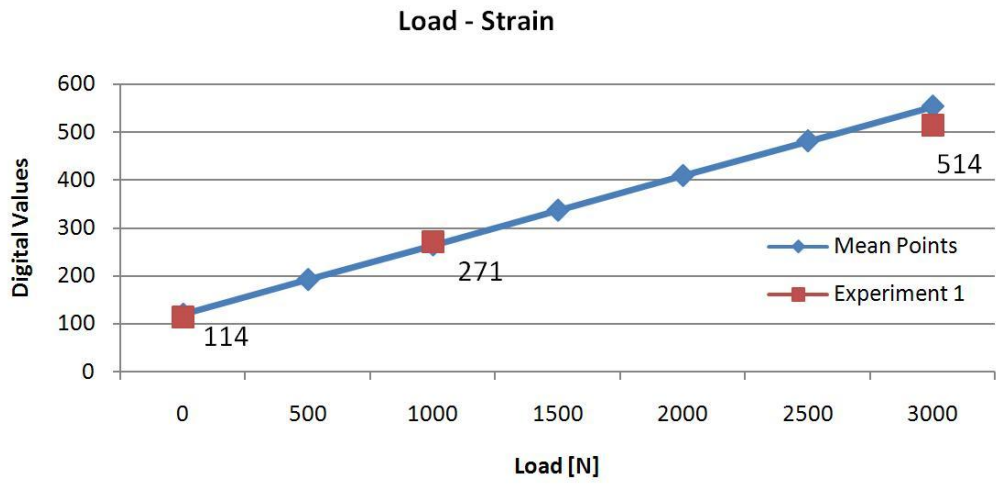


Figure 5.9 Comparison of experiment 1 values

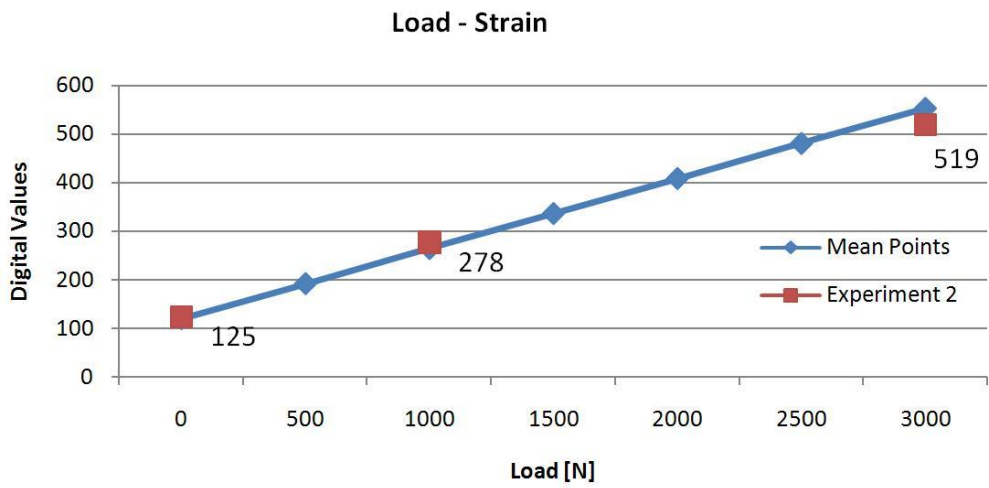


Figure 5.10 Comparison of experiment 2 values

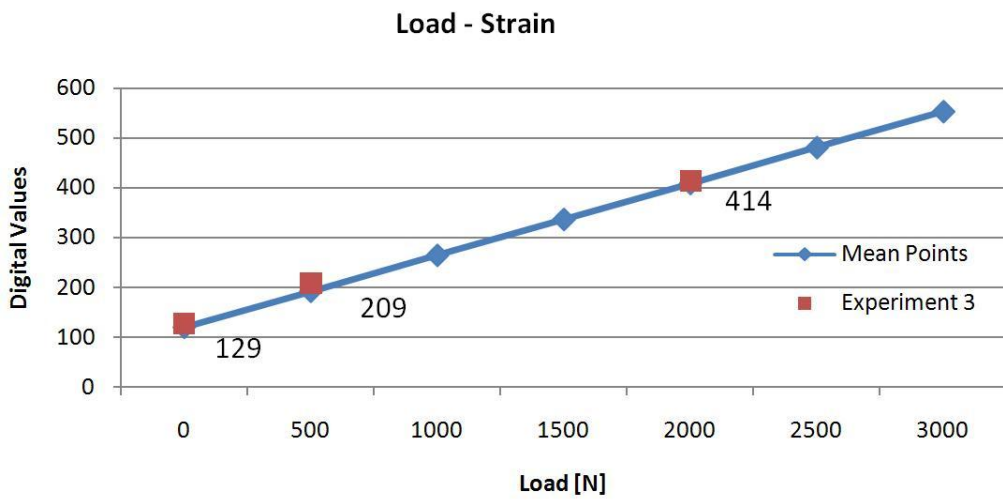


Figure 5.11 Comparison of experiment 3 values

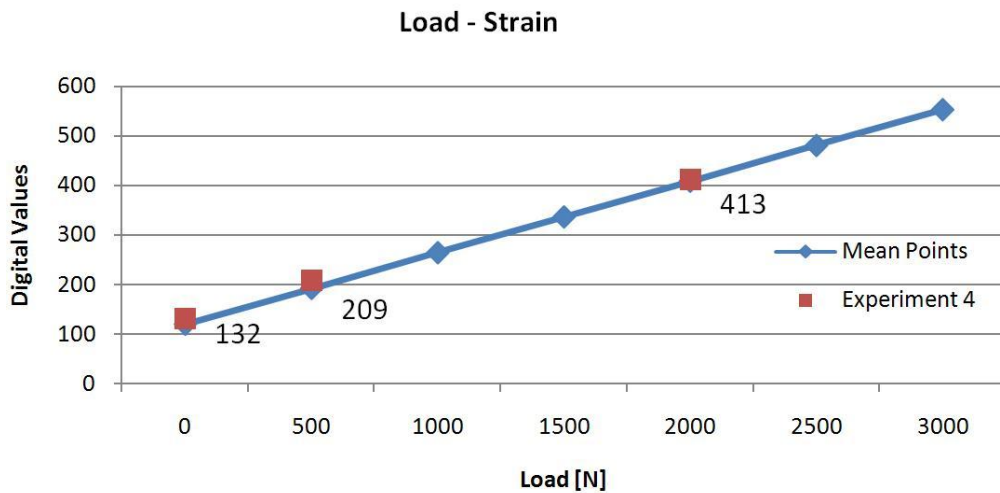


Figure 5.12 Comparison of experiment 4 values

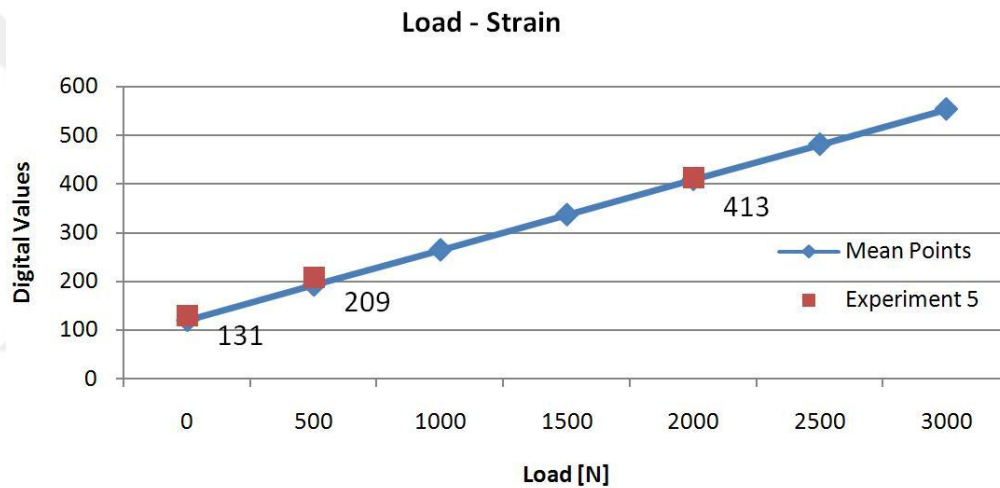


Figure 5.13 Comparison of experiment 5 values

After the experiments with the video extensometer, it was determined that these experiments were not suitable to calibrate the designed telemetry system. Strain data logger instrument was used to calibrate the system. Two periods of load between 500 N – 2000 N with load rate of 50N/s was applied two times each on the data logger and on the telemetry system by turns. In Figure 5.14 and Figure 5.15, the experiments' results with the data logger are given.

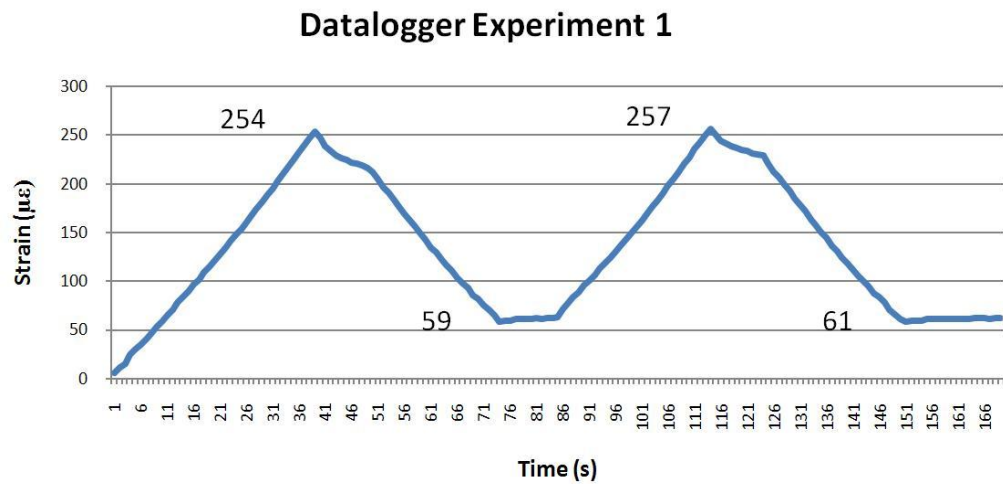


Figure 5.14 Result of experiment 1 with data logger

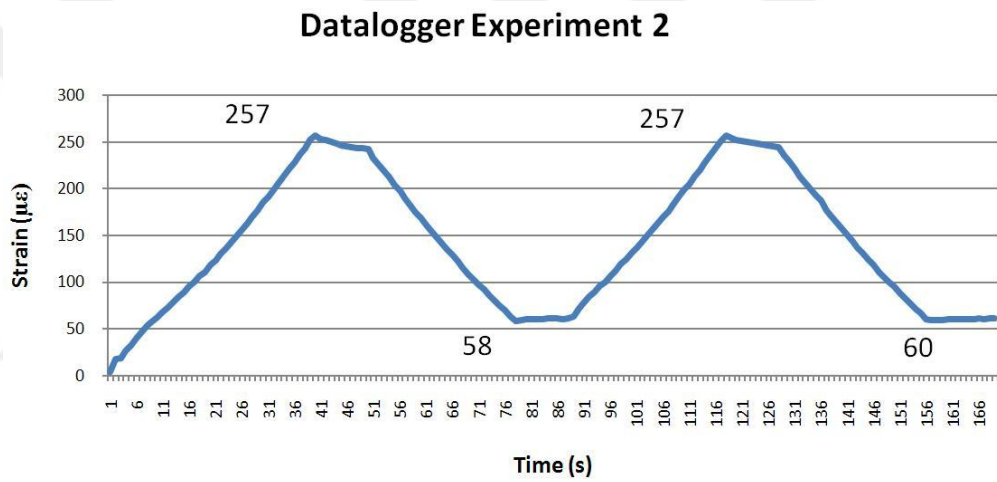


Figure 5.15 Result of experiment 2 with data logger

With the results of the experiments that were performed using data logger, the telemetry system was calibrated. The experiments' results that were performed using the calibrated telemetry system are given in Figure 5.16 and Figure 5.17. The calibration was performed by comparing the telemetry system's digital output which has the unit of bit [bit] and the output of data logger which has the unit of micro strain [$\mu\epsilon$]. As a result of the comparison the calibration number was found experimentally as 1.7751 [$\mu\epsilon/\text{bit}$]. Figure 5.16 and Figure 5.17 was formed by multiplying the digital outputs of the telemetry system with the calibration number.

Telemetry Experiment 1

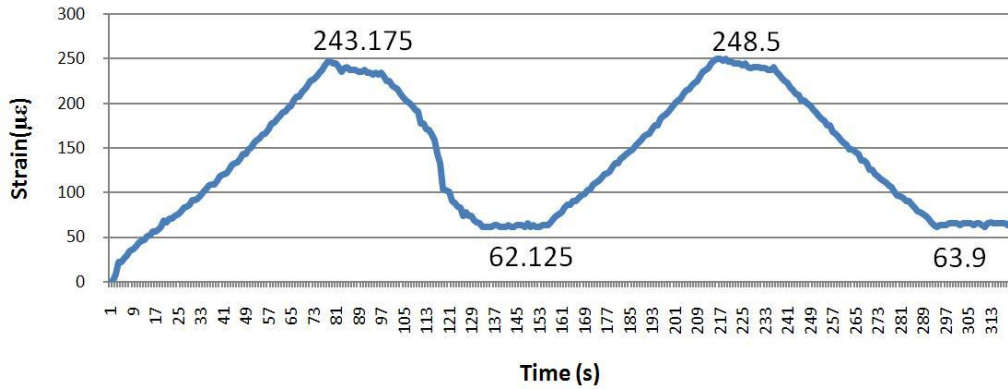


Figure 5.16 Result of experiment 1 with telemetry system

Telemetry Experiment 2

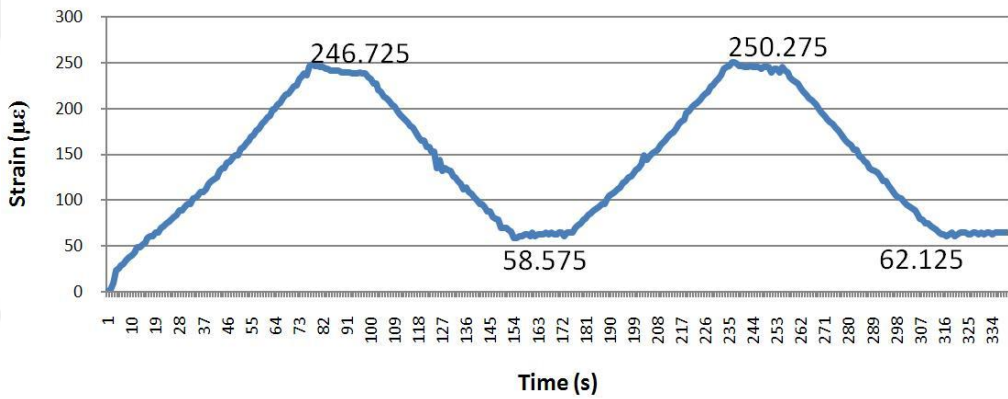


Figure 5.17 Result of experiment 2 with telemetry system

5.2 Tests on the Vehicle Rim

After the experiments in the laboratory the telemetry system was installed on a rim. Strain gage bridges were calibrated while the telemetry was connected to the rim. Strain gauges are placed on the rim in the form of quarter bridge type-II (Figure 5.18). As it is seen in Figure 5.18 one of the strain gauge is placed parallel to the direction of force acting on the rim and the other one which is called dummy is placed only for thermal compensation. Dummy strain gauge is not fixed on the rim with glue, there is thermal grease between the dummy strain gauge and the rim. Installation is shown in Figure 5.19.



Figure 5.18 Quarter bridge type-II installation of strain gauges



Figure 5.19 Installation of the transmitter circuit on the rim



Figure 5.20 Telemetry circuit and the rim is attached on the vehicle

Wheel was installed on the car and then 4 minutes long two tests were performed with the telemetry and the measurement data was logged in the computer. Logged data is shown in Figure 5.21 and Figure 5.22.

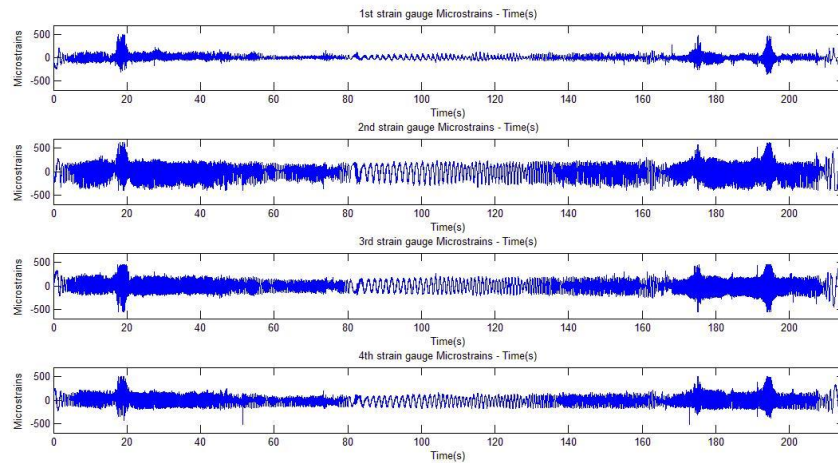


Figure 5.21 Strain data from the first experiment on the car

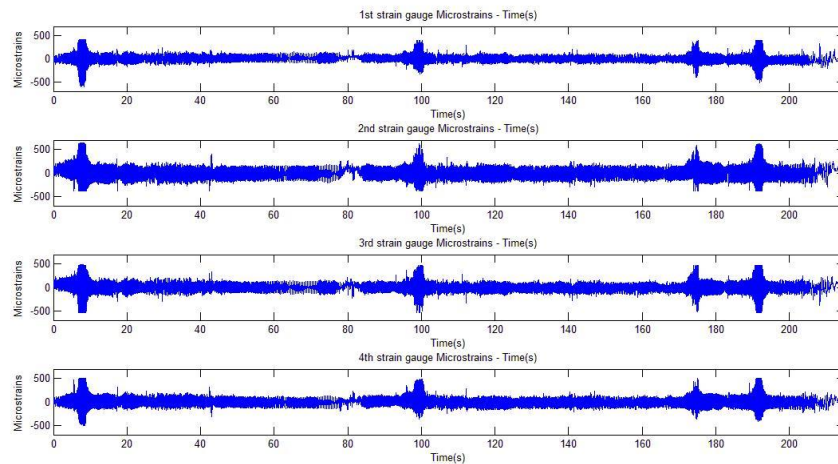


Figure 5.22 Strain data from the second experiment on the car

Strain gauges were installed on the rim with approximately 90 degrees of intervals. So, on the strain-time graphs phase difference of 90 degrees between strain signals can be seen. To be able to see the phase difference 2 seconds of data was zoomed in. The zoomed graph is given in Figure 5.23.

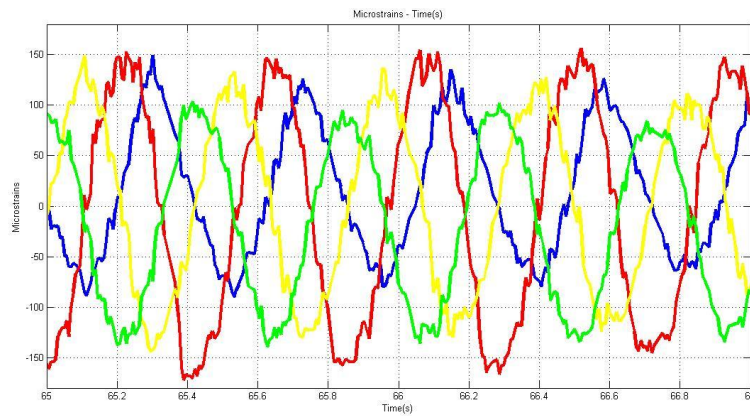


Figure 5.23 Phase difference between strain data

In Figure 5.21 it was seen that the first strain gauge's strain data was relatively lower than the other three strain gauges' strain data. After controlling the rim it was observed that the nut near the first strain gauge was tightened loosely. Before starting the second experiment, the loose nut was tightened. In Figure 5.22 it is seen that the first strain gauge's strain data is approximately at the same magnitude as the other three strain gauges' data.

CHAPTER SIX

CONCLUSION

In this research a wireless telemetry system for strain and acceleration measurements for a solar race car was designed produced and tested. Tests were performed both on universal test machine and vehicle rim. There is 2% difference between the calibration constants which were theoretically calculated and experimentally found. When the results of the experiments are analyzed it can be observed that applied loads and strain measurements are linear. According to the tests performed on the vehicle rim, the measurements are sensitive even for detecting the tightness of a rim's nut.

This research is supported by Ministry of Science, Industry and Technology of Republic of Turkey with the project number of 0065.STZ.2013-1 for CMS Jant ve Makina Sanayi A.Ş.. Purpose of the project was measuring the dynamic loads acting on vehicle rim wirelessly. The requirements of the project is fulfilled by this research.

REFERENCES

- Analog Devices. (2012). Wide supply range, rail-to-rail output instrumentation amplifier. *AD8226 datasheet, [Revision C]*.
- Analog Devices. (2008). Single-supply, rail-to-rail, low cost instrumentation amplifier, *AD623 datasheet, [Revision D]*.
- Arms, S.W., Townsend, C.P., Churchill, D.L., Hamel, M.J., Galbreath, J.H. & Mundell, S.W. (2004). Frequency agile wireless sensor networks. *In Proceedings of SPIE 5389, Smart Structures and Materials*. U.S.A., 5389.
- Blaisdell, G. L. (1983). The CRREL instrumented vehicle. *Cold regions research and engineering lab, Hanover, New Hampshire, United States, Technical Report*. AD-A128 713.
- Doherty, B. (2009). *Dynamic tire load acquisition for ground vehicle handling analysis with NI CompactRIO*. Retrieved January 27, 2015, from <http://www.ni.com/white-paper/9274/en/>.
- Erdogan, G., Borrelli, F., Tebano, R., Audisio, G., Lori, G. & Sannazzaro, J. (2010) Development of a new lateral stability control system enhanced with accelerometer based tire sensors. *In Proceedings of ASME Dynamic Systems and Control Conference '10*, 2, 841-848.
- Freescale Semiconductor. (2014). MMA8653 3-Axis, 10-bit digital accelerometer. *MMA8653 datasheet, [Revision 2.1]*.
- Gutiérrez-López, M. D., de Jalón, J. G. & Cubillo, A. (2015). A novel method for producing low cost dynamometric wheels based on harmonic elimination techniques. *Mechanical Systems and Signal Processing*, 52–53, 577-599.

- Kanehara, H., & Fujioka, T. (2002). Measuring rail/wheel contact points of running railway vehicles. *Wear*, 253 (1–2), 275-283.
- Karoumi, R., Wiberg, J. & Liljencrantz, A. (2005). Monitoring traffic loads and dynamic effects using an instrumented railway bridge. *Engineering Structures*, 27 (12), 1813-1819.
- Kester, W. (2005). Section 4-3 - Strain, force, pressure and flow measurements. *Op Amp Applications Handbook*. (edited by Walt Jung). (247-256). Burlington: Newnes.
- Kuchler, M., Meier, H., Nohl, F. & Camacho, D. A. F. (1999). *Wheel force measuring hub assembly*. U.S. Patent 5,894,094.
- Lagoda, T., Macha E. & Nieslony A. (2005). Fatigue life calculation by means of the cycle counting and spectral methods under multiaxial random loading. *Fatigue & Fracture of Engineering Materials & Structures*, 28 (4), 409-420.
- Lee, J.-S., Su, Y.-W. & Shen, C.-C. (2007). A comparative study of wireless protocols: Bluetooth. *In Proceedings of Industrial Electronics Society '07*. Taipei, 46-51.
- MTS. (2014). Flat-trac tire test systems. *Flat-Trac Catalog*.
- Murakami, Y., Mineki K., Wakamatsu T. & Morita T. (1999). Data acquisition by a small portable strain histogram recorder (mini-rainflow recorder) and application to fatigue design of car wheels. *European Structural Integrity Society, Elsevier*, 23, 135-145.
- Murakami, Y., Morita, T. & Mineki, K. (1997). Development and application of super-small size strain history recorder based on rainflow method. *Journal of the Society of Materials Science, Japan*, 46-10, 1217-1221.

- Murphy, E., & Slattery, C. (2005). *Direct digital synthesis (DDS) controls waveforms in test, measurement, and communications*, Retrieved June 26, 2015. http://www.analog.com/library/analogDialogue/archives/39-08/dds_apps.pdf
- Nagayama, T., Ruiz-Sandoval, M., Spencer Jr., B.F., Mechitow, K.A. & Agha, G. (2004). Wireless strain sensor development for civil infrastructure. *In Proceedings of 1st International Workshop on Networked Sensing System, U.S.A.*, 97-100.
- National Instruments. (2006). *Strain gauge configuration types*. Retrieved February 02, 2015. <http://www.ni.com/white-paper/4172/en/>.
- National Instruments. (2014). *Measuring strain with strain gages*. Retrieved Feb. 02, 2015. <http://www.ni.com/white-paper/3642/en/>.
- Nordic Semiconductor. (2007). Ultra low power 2.4GHz RF transceiver IC. *nRF24L01 datasheet, [Revision 2.0]*.
- Poussier, S., Rabah, H. & Weber, S. (2005) Adaptable thermal compensation system for strain gage sensors based on programmable chip. *Sensors and Actuators A: Physical*, 119 (2), 412-417.
- Pytko, J. A., Tarkowski P., Fijałkowski, S., Budzyński P., Dąbrowski J., Kupicz, W., et al. (2011). An instrumented vehicle for offroad dynamics testing. *Journal of Terramechanics*, 48 (5), 384-395.
- Texas Instruments. (2006). 0.9Ω low-voltage, single-supply, 4-channel SPST analog switch. *TS3A4751 datasheet, [Revision E]* (Revised January 2015).
- Thomas, J.J., Perroud, G., Bignonnet, A. & Monnet, D. (1999). Fatigue design and reliability in the automotive industry. *European Structural Integrity Society, Elsevier*, 23, 1-11.

APPENDICES

APPENDIX A: SOFTWARE OF TELEMETRY CIRCUIT

```
#include <htc.h>

#pragma config FOSC = INTIO67
#pragma config PLLCFG = ON
#pragma config PRICLKEN = OFF
#pragma config FCMEN = OFF
#pragma config IESO = OFF
#pragma config PWRTEN = ON
#pragma config BOREN = OFF
#pragma config BORV = 250
#pragma config WDTEN = OFF
#pragma config WDTPS = 512
#pragma config CCP2MX = PORTB3
#pragma config PBADEN = OFF
#pragma config HFOFST = OFF
#pragma config T3CMX = PORTC0
#pragma config P2BMX = PORTD2
#pragma config MCLRE = INTMCLR
#pragma config STVREN = OFF
#pragma config LVP = OFF
#pragma config XINST = OFF
#pragma config DEBUG = OFF
#pragma config CP0 = ON //CODE PROTECT
#pragma config CP1 = ON
#pragma config CP2 = ON
#pragma config CP3 = ON
#pragma config CPB = ON
#pragma config CPD = ON
#pragma config WRT0 = OFF // WRITE PROTECT
#pragma config WRT1 = OFF
#pragma config WRT2 = OFF
#pragma config WRT3 = OFF
#pragma config WRTC = OFF
#pragma config WRTB = OFF
#pragma config WRTD = OFF
#pragma config EBTR0 = OFF //TABLE READ PROTECT
#pragma config EBTR1 = OFF
#pragma config EBTR2 = OFF
#pragma config EBTR3 = OFF
#pragma config EBTRB = OFF

#include "pic_init.c"
#include "defines.c"
#include "mod.c"
#include "NRF2401.c"
#include "spi.c"
#include "adc_lib.c"
#include "str.c"
#include "i2c.c"
#include "aclmtr.c"

static void interrupt low_priority isr(void){
    if(RC1IF){
        get_data();
    }
}
```

```

        RC1IF=0;
    }
    if(TX1IF && TXSTA1bits.TXEN && TXSTA1bits.TRMT){
        send_data();
        TX1IF=0;
    }

    if(ADIF){
        ADIF=0;
    }
}

void main(void){
    unsigned char olcum_say=0, dly_i, tx_counter=0;

    //initialization part
    //-----
    pic_init();
    GIE=1;
    IPEN=1;
    PEIE=1;
    I2CInit();
    timer3_init();
    acclmtr_actv();
    SPI_Init();
    receive_init();
    adc_init();
    rf_adress=10;

    change_channel(rf_adress);
    gage_num=16;
    gain=16;
    //-----

    while(1){
        versiyon=813;

        PORTA=gage_num; //change selected strain gauge
        PORTD=gain; //set gain

        zaman=TMR3H*256+TMR3L; //get time in variable "zaman"
        for every measurement

        if(str_i==4)str_i=0; //change strain gauges in loop

            //After four strain gauges are measured
            //read accelerometer
            //and send wireless package
            //-----

        if(olcum_say>3){
            acclmtr(&acc_data);
            spi_transmit();

            tx_counter++;
            if(tx_counter>254)LED=!LED;

            olcum_say=0;
        }
    }
}

```

```

//-----

    for(dly_i=0;dly_i<4;dly_i++) //delay for settling of
instrumentation amplifier
    {
    delay();
    }

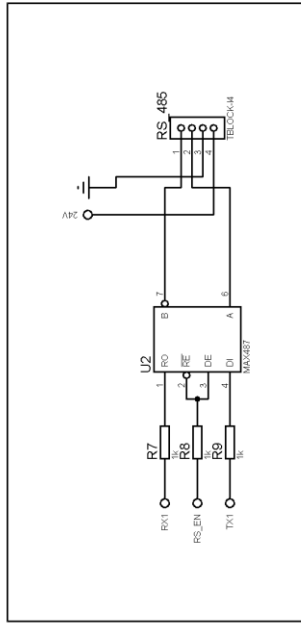
    read_str(); //measure strain gauges using ADC

    str_i++; //select next strain gauge
    olcum_say++;
}
}

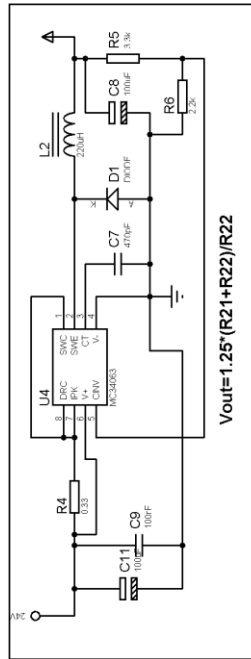
```



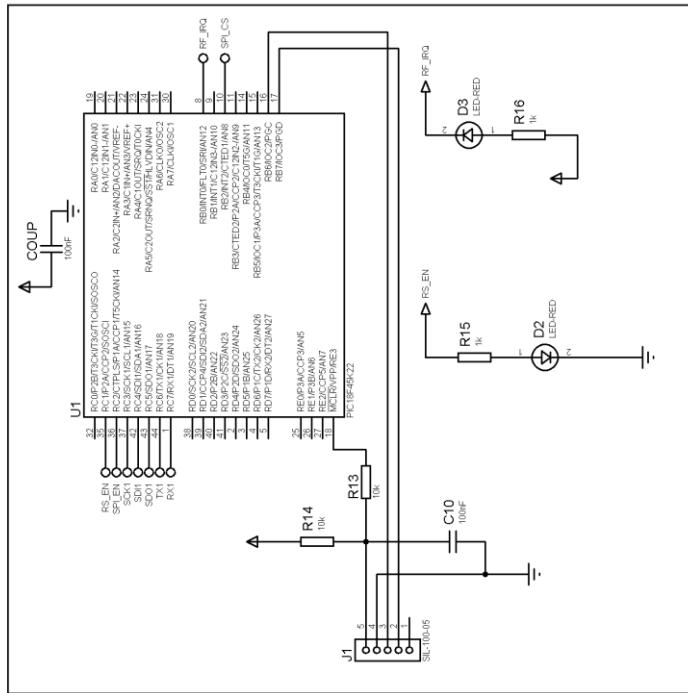
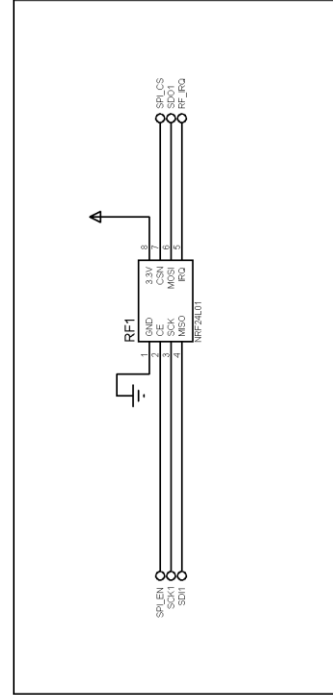
APPENDIX B: SCHEMATIC OF RECEIVER CIRCUIT



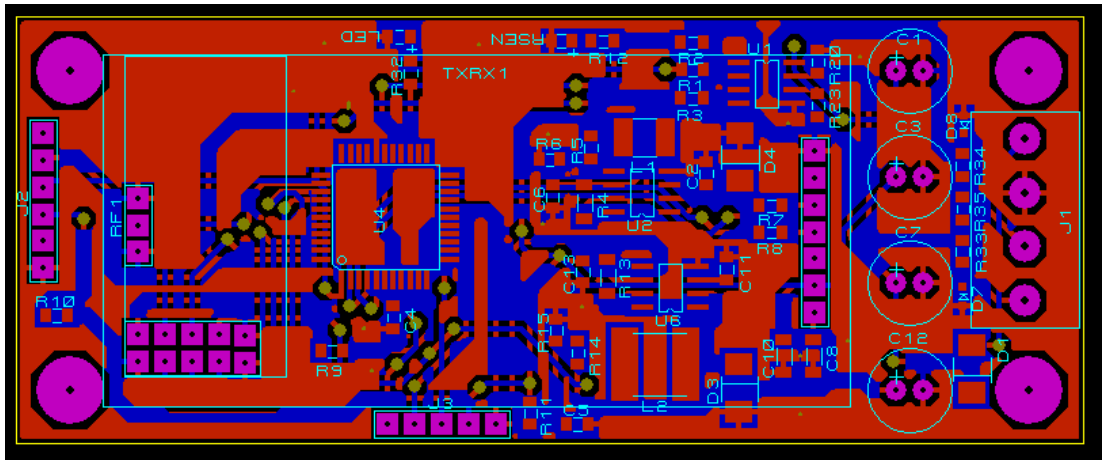
3.125V



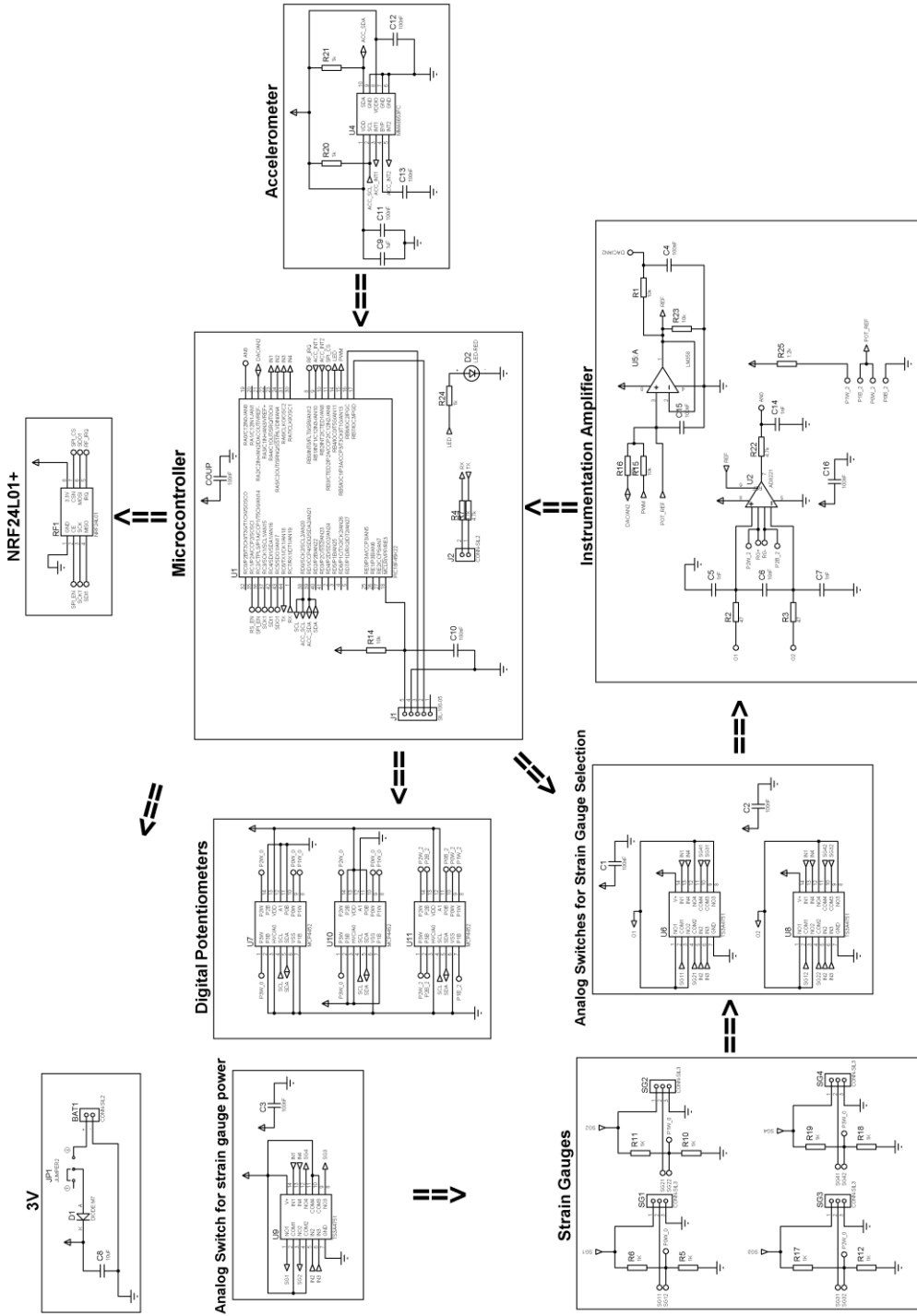
$V_{out} = 1.25 * (R_{21} + R_{22}) / R_{22}$



APPENDIX C: PCB LAYOUT OF RECEIVER CIRCUIT



APPENDIX D: SCHEMATIC OF TELEMETRY CIRCUIT



APPENDIX E: PCB LAYOUT OF TELEMETRY CIRCUIT

